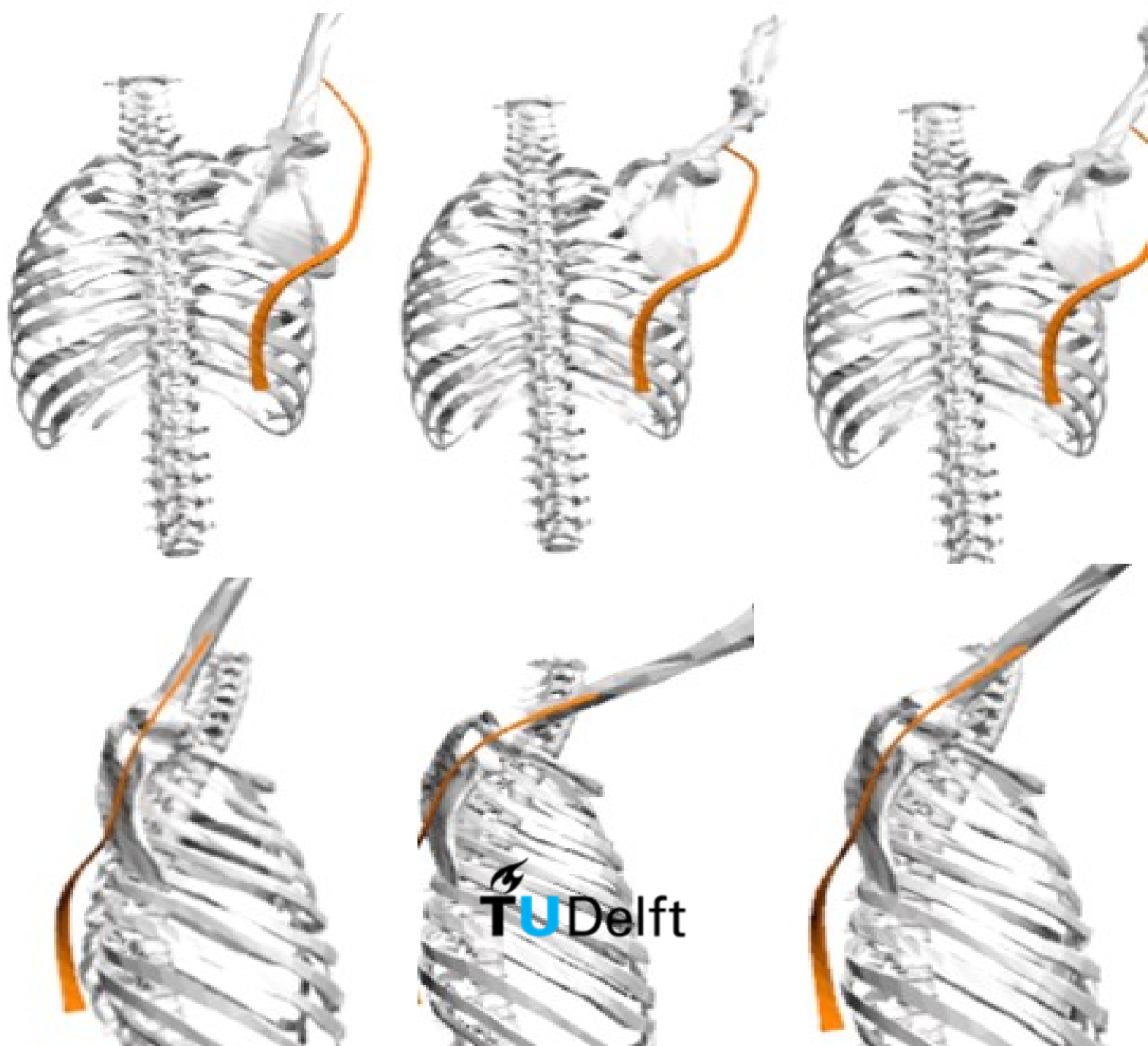


How Do Exoskeletons Change Shoulder Biomechanics?

A New Design Tool for “Human-In-the-Loop” Optimization of Shoulder Exoskeletons

MSc Thesis
Siyang Zhou



How Do Exoskeletons Change Shoulder Biomechanics?

A New Design Tool for “Human-In-the-Loop”
Optimization of Shoulder Exoskeletons

By

Siyang Zhou

To obtain the degrees of **Master of Science**
in Biomedical Engineering and Mechanical Engineering
at the Delft University of Technology
to be defended publicly on Monday December 18, 2023.

Thesis committee: Dr. ir. A. Seth, supervisor, TU Delft
Dr. ir. G. Radaelli, supervisor, TU Delft
Dr. ir. O. Nejadseyfi, TU Delft



Abstract

Shoulder exoskeleton is a popular solution to work-related shoulder disorders and muscle fatigue. With a wide range of exoskeletons designed, a comprehensive report on how the use of shoulder exoskeletons changes shoulder biomechanics is still missing. In this project, the impact of exoskeletons on shoulder biomechanics was investigated with the musculoskeletal simulation OpenSim. This study proposed a "human-in-the-loop" optimization-based design tool for shoulder exoskeletons. This design tool incorporates the predicted biomechanical effects of a shoulder exoskeleton from musculoskeletal simulations into design considerations. This design tool was validated with a case study designing a shoulder exoskeleton based on a compliant beam and testing the design in the musculoskeletal simulation and experiments.

The exoskeleton design tool is a coupling of finite element analysis and OpenSim. OpenSim calculates the deformation of the exoskeleton with human motion, and the finite element analysis calculates the force exerted from the exoskeleton upon deformation. Then OpenSim computes muscle activities under the external force from the exoskeleton. By merging muscle activities and the resultant glenohumeral joint reaction force to an objective function, the optimization-based design loop is closed by looking for the best objective value iteratively.

Several exoskeletons were designed by the new design tool to assist different types of tasks. The design tool exhibited good ability in finding optimal solutions for a range of design choices and design requirements. Simulated tests of designed exoskeletons showed significant effects on reducing muscle activities and good robustness in resisting the influence of perturbed motions in arm-elevated tasks. An exoskeleton was selected to be tested with an experiment set up in the same way as the simulated test. Experiment results supported the performance of the exoskeleton predicted in the simulated test.

This project established a method to comprehensively predict the effect of an exoskeleton on shoulder biomechanics and provided a more comprehensive understanding of biomechanical effects of shoulder exoskeletons. This facilitated the "human-in-the-loop" design process of shoulder exoskeletons which could greatly save money and time investments into prototyping, testing, and validation.

Acknowledgements

I have no idea who will, ever, read this acknowledgement, because this will not be publicly accessible until one year later, at least. I would assume those who typed my name in the search box of TU Delft repository at that time have quite some curiosity in the three years I spent in Delft.

Anyway, I have to write something now.

The beginning of my thesis work was very tough, I had to propose a topic myself, as no one knew how the two disciplines I was doing could be combined. After like four months I finally had an idea, the thing you are going to read later. Then things became enjoyable, I sat at home, drank coffee and coded, or watched the program running on its own while playing my violin. I would say the thing I “invented” worked so much better than I, or we, expected—it worked, instead of “after an extensive study on the proposed stuff, we concluded that it is not a viable solution”. This is also why this thesis will be embargoed. This is all I want to say about my thesis, because I believe I will do more impressive works in the future.

Then I am expressing my gratitude to some people, please imagine the scene of me in tear(not really). I first want to thank my parents for their unconditional and unlimited financial support and never asking me why I could not graduate on time. I am grateful for the guidance from my supervisors, Ajay and Giuseppe, they are encouraging and patient, and they tolerated my occasional burst of stupidity. I also want to thank my former daily supervisors, Sagar and Ali, as well as the PhD candidates who gave me a lot of help in the experiment. Last but not least, I would like to thank my friends for sharing all the good and bad moments with me, my life gets much easier with you.

Siyang Zhou
December 10, 2023

Contents

Abbreviations	iv
List of Figures	v
List of Tables	vi
1.Introduction	1
2.Methods	3
2.1 Predicting the biomechanical effects of an exoskeleton.....	3
2.2 Optimizing the design of exoskeletons.....	4
2.3 Evaluation criteria for exoskeleton designs.....	5
2.4 Design Case Study: Topology of the shoulder exoskeleton	8
2.5 Testing designed exoskeletons in the musculoskeletal simulation.....	11
2.6 Validating the exoskeleton design tool with experiments	11
3.Results	15
3.1 Performance of designed exoskeletons.....	15
3.2 Change in muscle activities with designed exoskeletons, 2kg-loaded and unloaded tasks	17
3.3 Robustness of the design	21
3.4 Experiment results.....	22
4.Discussion	25
4.1 Performance of design results	25
4.2 Difference between predicted change in muscle activation and EMG results.....	26
4.3 Further validation of the design tool.....	26
4.4 Limitation of the design tool and recommendation on future development.....	26
5.Conclusion	28
References	29
Appendix I. Implementation	31
Appendix II. Dimension of exoskeleton beam designs	34
Appendix III. Effects of exoskeleton-equivalent forces from design 2 on a male shoulder model	36

Abbreviations

EMG	Electromyography
RMR	Rapid Muscle Redundancy (solver)
FEA	Finite Element Analysis
MVC	Maximum Voluntary Contraction
EXO	Exoskeleton
noEXO	no-Exoskeleton
HREC	Human Research Ethics Committee

List of Figures

1.1 Left-Paexo Shoulder, middle-H-VEX, right-Tschiersky's compliant shoulder exoskeleton	1
2.1 Method to predict the biomechanical effects of an exoskeleton with simulation, the enclosed part is called the predictor of the exoskeleton's biomechanical effects	3
2.2 Schematic illustration of the compliant beam-based exoskeleton	4
2.3 Schematic illustration of "human-in-the-loop" exoskeleton design procedure	4
2.4 The musculoskeletal model of the shoulder with muscles actuating shoulder movements	5
2.5 Cylindrical space representing the upper arm	6
2.6 Markers in the OpenSim model construct triangles defining the shape of the back	6
2.7 Flowchart to detect interference between point p1 on exoskeleton and triangle area ΔTi on the back	7
2.8 Complete structure of the exoskeleton design tool, merging all evaluation criteria	8
2.9 The forces and moments that exoskeleton should exert on the user via two interfaces	9
2.10 The location of the lower back interface can be changed by a servo motor upon arm posture change	10
2.11 Left: arm postures in overhead work. Right: arm postures in full range of motion work	11
2.12 Left: schematic sketch of the experiment setup. Right: experiment setup in practice	12
2.13 Design of the arm cuff	12
2.14 EMG electrodes attachment	13
3.1 Exoskeleton design 2 on musculoskeletal model in initial posture and arm posture 1-3	16
3.2 Exoskeleton design 5 on musculoskeletal model in initial posture and arm posture 1-5	17
3.3 (a-c) Muscle activities in arm posture 1-3 with and without the exoskeleton design 2	18
3.4 (a-e) Muscle activities in arm posture 1-5 with and without the exoskeleton design 5	21
3.5 Change of total muscle activation with motion perturbation, design 2, arm posture 1-3	22
3.6 Change of total muscle activation with motion perturbation, design 5, arm posture 1-5	22
3.7 (a-c) Muscle activities of participants 1-3 with and without the exoskeleton-equivalent forces from design 2 of arm posture 1-3	24
D1 Calculate beam deformation with the FEA	31
D2 Effects of exoskeleton-equivalent forces from design 2 on a male shoulder model	36

List of Tables

3.1. Description of each design.....	15
3.2. Main performances of the designs	15
D1. Dimensions of exoskeleton beam designs.....	34
D2. Dislocation of lower back interface by servomotor per arm posture	35

1

Introduction

Shoulder exoskeletons have been proposed as a solution to work-related fatigue and shoulder musculoskeletal disorders over the years[1]. Many shoulder exoskeletons have been designed to provide assistance for overhead work. Representative products include Paexo Shoulder by Ottobock Corporate[2] and COMAU MATE[3]. As occupational shoulder exoskeletons are expected to be widely equipped for industrial workers, the cost of exoskeletons is a major concern. For this reason, most occupational shoulder exoskeletons have opted for a passive mechanism. The motor-less feature not only reduces the cost but also minimizes the volume and mass of the exoskeleton, with the added advantage of eliminating the need for charging. Passive shoulder exoskeletons often use springs to store and release energy. A leverage or a gearbox is then employed to convert the force from the spring into torque, countering the effects of gravity on arms. In addition to these mechanisms, some studies have explored the use of compliant mechanisms in exoskeleton design. Tschiersky employed a shape-optimized compliant beam to provide optimal support in various arm postures[4], significantly reducing the structural complexity of the exoskeleton. Compared to traditional mechanisms, compliant mechanisms have emerged in exoskeletons relatively recently and remain underexplored.



Figure 1.1. Left-Paexo Shoulder[2], middle-H-VEX[5], right-Tschiersky's compliant shoulder exoskeleton[4]

Occupational shoulder exoskeletons are typically designed for overhead tasks such as automotive manufacturing and window or ceiling cleaning. To evaluate the effectiveness of exoskeletons, surveys have been conducted with industrial workers participating in shoulder exoskeleton trials. These surveys inquire about the reduction in perceived fatigue and the willingness to continue wearing exoskeletons. In recent years, numerous studies have incorporated biomechanical measurements, such as electromyography and motion tracking, to objectively assess the impact of exoskeletons on muscle activities and movements. Usually, the concern lies more with muscle activities, as they reflect the stress in muscles and predict whether wearing the exoskeleton reduces muscle fatigue. Reduced activities in deltoids, trapezius, biceps, and latissimus dorsi have been reported in many

1. Introduction

studies[6, 7], but certain muscles, specifically the rotator cuff group have been rarely or never included in muscle activity measurements during exoskeleton evaluations. The rotator cuff group includes infraspinatus, supraspinatus, subscapularis, and teres minor, and they play a very important role in stabilizing the humerus[8]. Their activities are difficult to measure with surface electromyography as they are deep beneath the skin.

The absence of measurements for activities in the rotator cuff group introduces uncertainties about whether wearing exoskeletons can effectively reduce stress and fatigue in shoulder muscles. Although measurable shoulder muscles may show reduced activities, those unmeasured shoulder muscles may have increased activities after wearing exoskeletons, and this is called muscle compensation. Increased activities in muscles such as biceps, upper trapezius, and latissimus dorsi have been reported[9], raising reasonable concerns about potential muscle compensation in the rotator cuff group.

Another unmeasured effect in exoskeleton evaluation is the joint load. The joint load is the reaction force to forces in muscles around the joint and external loads acting on adjacent segments. A large joint load may increase the risk of cartilage damage and other musculoskeletal disorders. Joint loads are often measured in subjects with instrumented prosthesis, but these subjects have never been involved in exoskeleton evaluations. It is plausible that a shoulder exoskeleton may induce a large load in glenohumeral joint while reducing muscle activities, especially when the exoskeleton exerts force along the humerus direction into the glenohumeral socket. Using such a shoulder exoskeleton will harm shoulder wellness, but the current evaluation of exoskeletons cannot measure if an exoskeleton induces a large load in the shoulder.

Considering these unmeasurable effects of exoskeletons, shoulder biomechanics may not be adequately considered in the design process of shoulder exoskeletons. Typically, the effects of an exoskeleton on shoulder biomechanics are evaluated post-design with a prototype. This implies that the design and testing of shoulder exoskeletons are time-consuming and costly, and certain biomechanical effects may be overlooked until the testing phase or even remain unclear.

Biomechanical effects of exoskeletons that are challenging to measure experimentally can be assessed through musculoskeletal simulations, such as OpenSim[10] and AnyBody[11]. Van der Have et al[12] and Gillete et al[13] modeled exoskeleton-assisted overhead work in OpenSim and Anybody, respectively, both reporting a decrease in glenohumeral reaction force. Despite their potential, these studies did not report computed shoulder muscle activities and therefore did not reveal activities in the rotator cuff group. Nevertheless, they demonstrated the viability of using musculoskeletal simulations to reveal unmeasurable biomechanical effects of exoskeletons.

Building on the potential demonstrated in musculoskeletal simulations, this study proposed a "human-in-the-loop" optimization-based design tool for shoulder exoskeletons. This design tool incorporates the predicted biomechanical effects of a shoulder exoskeleton from musculoskeletal simulations into design considerations. To validate this design tool, a case study was conducted, designing a shoulder exoskeleton based on a compliant beam. This exoskeleton was then tested in musculoskeletal simulations and experiments.

This report first presented the methodology of this study, which covered the theoretical background and technical details of the proposed exoskeleton design tool, as well as design considerations and testing methods of the case study. The results section presented shoulder exoskeletons designed by the proposed design tool, along with their performances in the musculoskeletal simulation and experiments. The performances of designed exoskeletons were reflected in the reduction of shoulder muscle activities and glenohumeral joint reaction forces compared to a no-exoskeleton scenario. In the discussion, the performances of the designed exoskeletons were reviewed, and the limitations of the proposed design tool revealed in the case study were emphasized.

2

Methods

The first half of the method section is about the structure, theoretical backgrounds, and technical details of the proposed exoskeleton design tool. The key point of the structure is the coupling of the finite element analysis and the musculoskeletal simulation OpenSim, which computes the biomechanical effects of an exoskeleton. Then it is introduced how this coupling can further become a design tool of exoskeletons with optimization. To support the choices on design objectives, theoretical backgrounds of shoulder disorders are provided. A method to rapidly check interference between the exoskeleton and the human body is also introduced here.

The second half of this section introduces the case study. First, the topology of the exoskeleton to be designed is determined and reasoned, and the tasks to be assisted by the exoskeleton are introduced. Then, the method to test the performance of the designed exoskeleton in OpenSim is explained. The last part is the introduction to experiment setups and procedures.

2.1 Predicting the biomechanical effects of an exoskeleton

To evaluate the biomechanical effects of an exoskeleton, information of muscle activation and joint reaction force while performing some movement/postures with the exoskeleton is required. As it is not possible to obtain this information from experiments, the biomechanical simulation software OpenSim[10] is used.

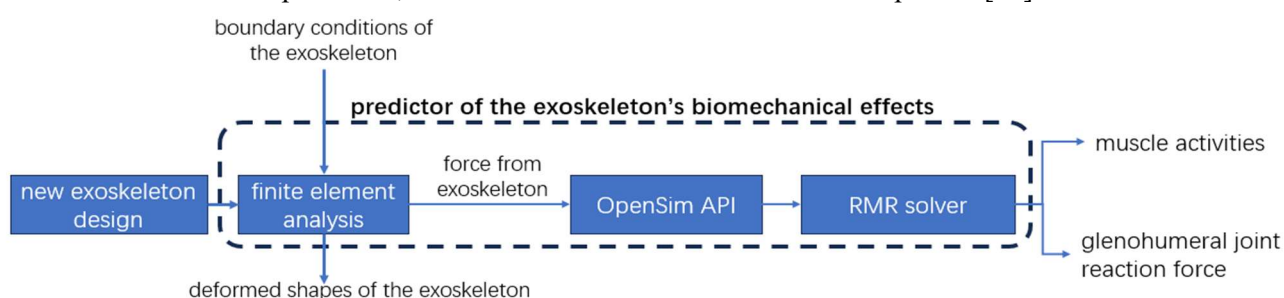


Figure 2.1. Method to predict the biomechanical effects of an exoskeleton with simulation, the enclosed part is called the predictor of the exoskeleton's biomechanical effects.

Due to the redundancy in the musculoskeletal system, muscle activities cannot be directly solved from movements by inverse dynamics. To deal with muscle redundancy, an optimization is performed in each time frame of movement to minimize the total muscle activation that can achieve this movement status, subject to a constraint on the direction of joint reaction force and the maximum level of muscle activities. This procedure is performed by the rapid muscle redundancy (RMR) solver with OpenSim MatLab API[14]. Inputs of this procedure include the movement of joints of interest, in format of either motion capture marker data or joint angles processed from marker data, and external forces if applied. Outputs are muscle activities and reaction forces in joints of interest in each time frame of the analyzed movement.

2.2. Optimizing the design of exoskeletons

The assistive force from the exoskeleton varies in each arm postures as locations of the interfaces between the exoskeleton and the user change and the exoskeleton deforms. Therefore, the assistive force can be calculated for each posture of the user, as long as the relation between the user's posture and the position of the exoskeleton's interfaces is known. In this specific design case of a compliant beam-based exoskeleton, we use a finite element analysis (FEA) MatLab script using beam elements[15] to calculate the assistive force from the deformation, caused by dislocations of the beam's two interfaces relative to each other.

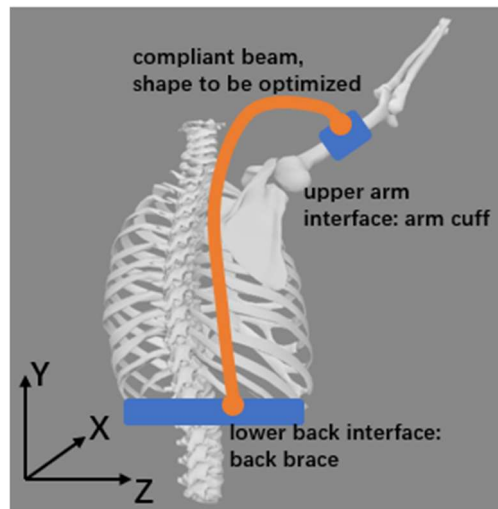


Figure 2.2. Schematic illustration of the compliant beam-based exoskeleton.

To simulate an exoskeleton-assisted movement, an experimentally recorded motion file of this movement without an exoskeleton is needed. In this project the motion data collected by a previous OpenSim project is used[16]. In each time frame of the movement, the position of interfaces of the exoskeleton can be retrieved from the motion file, as the interfaces between the exoskeleton and the user are represented by markers on the human model. By applying dislocations of interfaces' position as boundary conditions, the FEA calculates the reaction force from the exoskeleton in each time frame. This assistive force is the input to the RMR solver as an external force together with the motion file. The RMR solver then outputs muscle activities and joint reaction forces in this time frame of movement. With these outputs, a criterion representing the biomechanical effect of the exoskeleton can be set up.

2.2 Optimizing the design of exoskeletons

The method to predict the biomechanical effect of an exoskeleton can facilitate an optimization-based design procedure of shoulder exoskeletons that takes muscle activities and joint reaction forces as main design considerations. With the muscle activities and joint reaction forces in the glenohumeral joint, the assistive performance of the exoskeleton can be evaluated with some criteria, which can be merged into design objectives of this exoskeleton. By optimizing design objectives iteratively, the design of the exoskeleton can be updated, and an optimal design under the exoskeleton's evaluation criteria can be eventually found (figure 2.3).

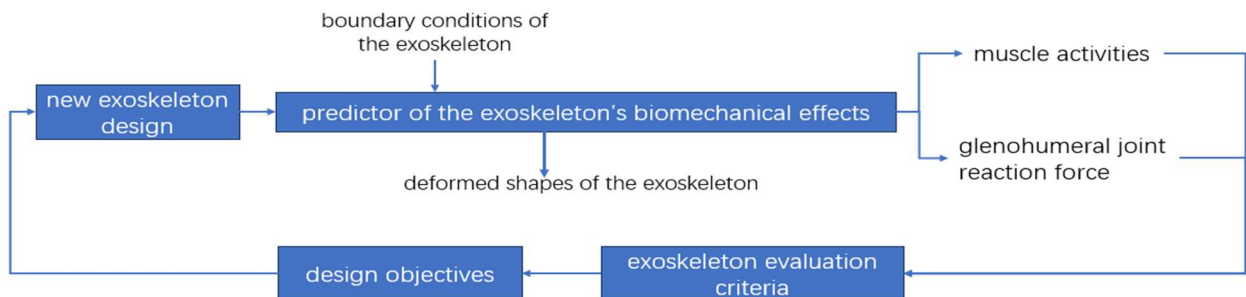


Figure 2.3 Schematic illustration of “human-in-the-loop” exoskeleton design procedure.

2.3 Evaluation criteria for exoskeleton designs

2.3.1 Evaluating the biomechanical effects

The biomechanical effect of an exoskeleton should consist of the effect on muscle fatigue, muscle health, and joint health. Reducing muscle fatigue is the primary purpose of occupational exoskeletons, and it can be reflected by the reduction in the total muscle activation compared to the no-exoskeleton scenario. Fatigue in an individual muscle may happen if its activity increases significantly despite the total muscle activation decreasing with an exoskeleton. Another possible drawback of this possibility is that the user may have a hard time getting used to the exoskeleton as the muscle activation pattern now deviates from the no-exoskeleton scenario. Therefore, an increase of 20 %MVC or larger in the activity of any individual muscle is taken as a negative effect in this criterion, regardless of the decrease in the total muscle activation.

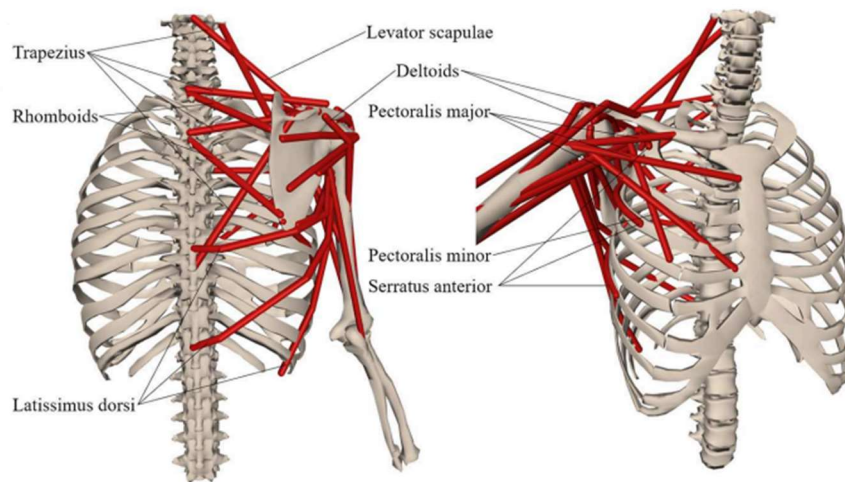


Figure 2.4. The musculoskeletal model of the shoulder with muscles actuating shoulder movements[16].

Muscle health will be at risk when muscle strain increases under excessive stress in the muscle[17]. Chronic muscle pain will also present if muscles are overused, which is moderately high muscle stress lasting for a long time. Considering the occupational usage of most shoulder exoskeletons, it is determined that the maximum level of activity in any muscle should not exceed 30 %MVC as a threshold indicating there is no excessive stress in muscles in the scenario of long-time work. It should be noted that no quantitative relations between the level of muscle activities and muscle fatigue or muscle health has been found in literature. Instead, the thresholds established here were estimated with previously reported activities in shoulder muscles during unloaded arm movements, and the thresholds were set slightly lower than the actual level of muscle activities due to the observation that OpenSim and RMR solver have the tendency to underestimate muscle activities[14, 16].

In musculoskeletal simulations, joint conditions can be described by the magnitude and direction of joint reaction forces. A high joint reaction force may correlate to narrowing of joint spaces and cause chronic damage to cartilages, while a certain level of joint reaction force is necessary for joint health. However, there is no sufficient study revealing what levels of joint reaction forces can be harmful. In this study, a reference was temporarily set to be the level of joint reaction forces in the no-exoskeleton scenario. If wearing an exoskeleton results in a joint reaction force larger than this reference level, the effect of this exoskeleton on joint health is considered negative. When the direction of joint reaction force is not pointing into the joint socket, the joint has a tendency of dislocation, and cartilages and ligaments may tear. Nevertheless, the evaluation criterion does not need to include this, as the RMR solver includes the constraint on the direction of joint reaction force, and when it gives a feasible solution to muscle activities, the direction of joint reaction force points into the joint socket.

2.3. Evaluation criteria for exoskeleton designs

When the RMR solver cannot give a feasible solution, it means the assistive force from the exoskeleton may cause unbearable effects on the user, and the evaluation criterion takes this as a highly negative effect.

Another negative effect by the exoskeleton could be that the assistive force from the exoskeleton has a large fraction along the humerus and causes slip or uncomfortable friction on the arm interface. Minimal fraction of the assistive force along the humerus can be an additional design concern. However, it was not clear before the design procedure if the design tool will compromise assistive effects of the exoskeleton to achieve this design concern that is not as critical. Therefore, two exoskeletons, one with this design concern and the other without it, should be designed with the design tool, and this design concern can be kept if the assistive effects are not much compromised.

2.3.2 Detecting interference between the exoskeleton and human body

The commonly used method in the previous study to measure interferences between a wearable device and the user is to detect interferences between the device shape and a mesh representing the user[4]. However, in an iterative optimization design process, using a mesh will make the program more computationally expensive. Also, as users of the exoskeleton can vary from the OpenSim model used in this design tool, it is not very beneficial to depict the body shape of the user in a very detailed way. Therefore, a simpler way to measure interferences is introduced here.

The area of human body where interferences with the exoskeleton may occur includes back and upper arm on the wearing side. The upper arm of the user is represented by a cylinder capped with two half spheres defined by humerus head marker and elbow center marker in the OpenSim model, with radius representing the thickness of upper arm. Interferences between the exoskeleton and upper arm will be detected if any point on the exoskeleton is in the cylindrical space. As the upper arm interface is defined at the mid-point of the humerus, the first 5 points next to the upper arm interface are always in this cylindrical space and should be thus excluded from interference check.

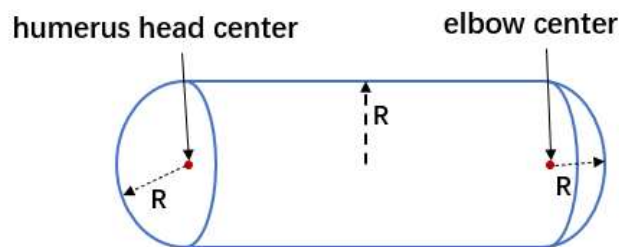
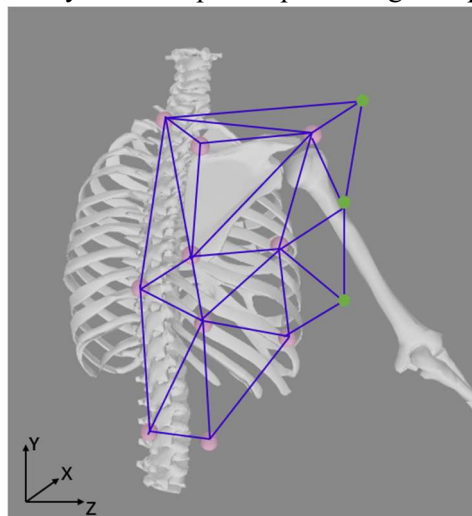


Figure 2.5. cylindrical space representing the upper arm



2.3. Evaluation criteria for exoskeleton designs

Figure 2.6. Markers in the OpenSim model construct triangles defining the shape of the back. Pink dots are the markers on the OpenSim model, and green dots are points far in the +X direction used to construct the lateral side of the torso.

The shape of the back changes apparently with arm elevation movement, so some markers from the motion file are selected to construct a surface representing the back. The shape of the upper back is described by 3 markers on the scapula and 1 marker on cervical spine, as shape change of the upper back is mainly caused by the movement of the scapula during high arm elevation. Shape of the lower back is defined by 2 markers on the spine, 2 markers on the spinal erector, and 2 markers on the lateral side of the back. The anterior part of the torso is not constructed, instead, the lateral side of the torso is extended remotely along +X direction with some reference points (the green dots in figure 2.6), as the exoskeleton is not supposed to go around the torso and go to the front of user, which is indicated by the exoskeleton intersecting with the lateral part of the torso. With these markers, the shape of the back and lateral torso is defined by a set of triangles constructed by the markers (figure 2.6), and each triangle is denoted as ΔT_i . To detect interference between a point p_1 on the exoskeleton and the back, a reference point p_2 is set on the anterior side of the back. If p_1 does not have interference with the back, the line connecting p_1 and p_2 , $\overline{p_1p_2}$ must penetrate odd numbers of triangles on the back (figure 2.7). A loop runs through every element of the FEA model of the beam part of the exoskeleton in its deformed shapes, checking its interference with the back and the upper arm cylinder. As each element has a rectangular cross section, the 4 vertices of the rectangle are checked individually. The two interfaces between the exoskeleton and the user, like the arm cuff and the lower-back brace, are excluded from interference check, as the contact cannot be modeled with the FEA.

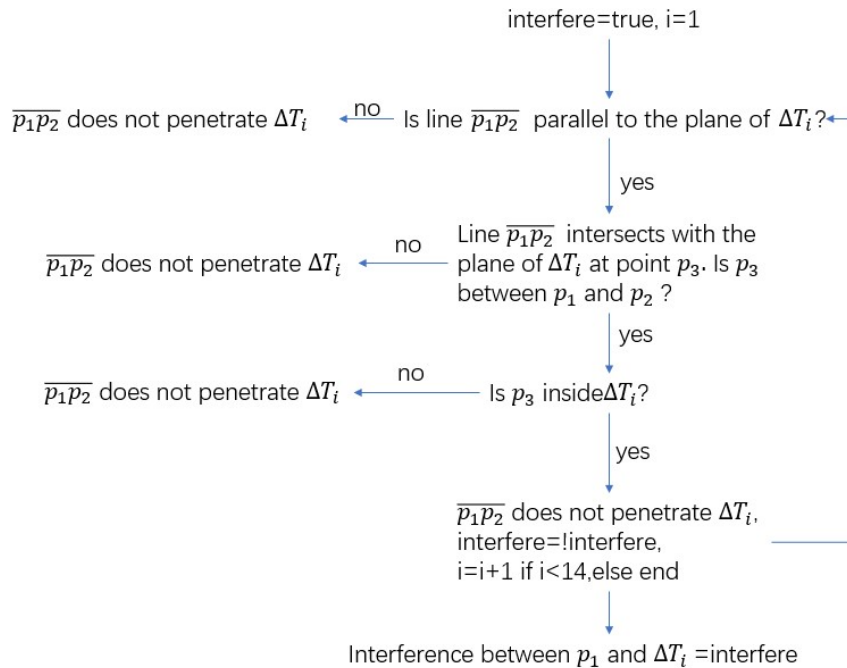


Figure 2.7. Flowchart to detect interference between point p_1 on exoskeleton and triangle area ΔT_i on the back.

In principle, detection of interference between the exoskeleton and the user should be a constraint on the optimization, because there should be no interference at all. However, it was found in practice that implementing it as a constraint made the optimization difficult for the solver and feasible solutions may not be found. This constraint would be highly nonlinear if implemented, as the deformation of the exoskeleton is nonlinear. In this project, detection of interference is implemented as a part of the penalty and the weight of this part is very large, so interference is guaranteed to be zero in found solutions.

2.3. Evaluation criteria for exoskeleton designs

2.3.3 General constraints in beam shape optimization

Apart from the specific design purpose of this exoskeleton, some general constraints apply in the optimization of compliant beams. When a compliant beam is deformed as required by design purposes, the internal strain of the beam should be within its recovery range, otherwise material failure may happen. In this design tool, a method developed in previous work[18] is employed. Similar to the constraint on interference, this constraint on the internal strain is also implemented as a part of the penalty with a high weight, as it is also a nonlinear constraint with FEA computation.

Bernoulli beam assumption is used in the development of the FEA in this design tool, and the calculation is only accurate for slender beams where shear deformation can be neglected. Therefore, the relative thickness of the compliant beam, the main body of the exoskeleton, to its length should also be constrained. There is no specific threshold for the ratio between beam thickness and length that is suitable for Bernoulli beam assumption. Referring to previous works[4, 15] and considering the total length of this exoskeleton, the maximum thickness of the beam is 30mm, set as a limit on optimization variables.

2.3.4 Complete structure of the exoskeleton design tool

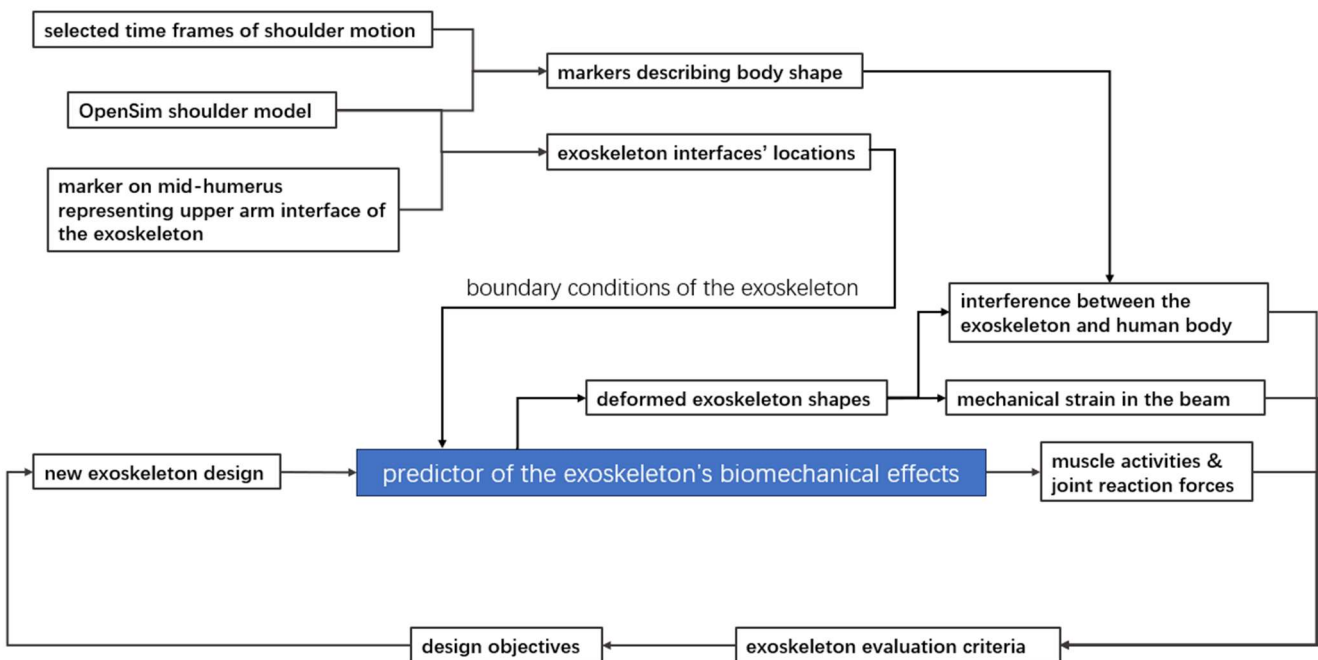


Figure 2.8. Complete structure of the exoskeleton design tool, merging all evaluation criteria.

2.4 Design Case Study: Topology of the shoulder exoskeleton

The primary purpose of the case study is to evaluate the design capability of the proposed exoskeleton design tool. By examining the performance of the resultant design, it can be suggested whether the design tool can find a feasible exoskeleton design with a more realistic modeling of the shoulder biomechanics and manage various design requirements. Investigating the use of a servo motor in the exoskeleton examines the capability of the design tool in modeling different mechanical designs. The exoskeleton is also optimized for two different working scenarios, to support the design tool's ability in designing exoskeletons for different purposes. Methods to evaluate the performance of the resultant designs include using the musculoskeletal simulation and conducting an experiment, as introduced in section 2.5 and 2.6.

2.4. Design Case Study

2.4.1 From 2D to 3D exoskeleton shape

Design of a compliant beam-based arm exoskeleton was only explored in planar mechanism designs [4]. When a more realistic shoulder biomechanics is considered, a planar beam shape is no longer sufficient for design requirements due to following reasons.

- 1) Although arm elevation mainly moves in a vertical plane, it is not planar. Wearing an exoskeleton designed in a planar space will impose some unpredicted out-of-plane deformation to the exoskeleton, and extra reaction forces will be thus generated.
- 2) When the beam shape is in a plane aligned with the plane of arm elevation, it must go above the shoulder from the user's posterior area and reach the anterior side of the upper arm to avoid interference with the user. This kind of beam shape will be subject to large deformation with the arm's movement, and the internal strain can easily go beyond the constraint mentioned in 2.3.3.
- 3) When the beam shape follows the path described in 2), large protrusion over the user's shoulder also occurs. This can be observed in the design results of previous work[4]. Large protrusions should be avoided in designs of exoskeletons, as it may impose inconvenience to users.

Due to these reasons, this case study explores beam shapes in the 3D space.

2.4.2 An initial analysis of interface connection mechanisms

The boundary conditions to compute deformation of the exoskeleton in the FEA are formulated by the locations of exoskeleton interfaces and connection mechanisms between the exoskeleton and the user at interfaces, e.g., via a ball joint, a hinge joint, a clamp, etc. Connection mechanism determines the degree of freedom of the exoskeleton and therefore affects its mechanical behavior. The exoskeleton is connected to the user via two interfaces, one on the lower back and the other on the mid-point of the upper arm. The position of the upper arm interface is coupled to a bone marker in the OpenSim model, while the position of the lower back interface can be optimized within a range. There can be many combinations of connection mechanisms, but many of them can be exempted after a very initial analysis of different boundary conditions' physical properties.

- 1) The connection on the upper arm interface must be torque-free, like a ball joint, as applying torque to a rather small interface on the human body can be uncomfortable.
- 2) The lower back interface should not translate freely in any direction, as in this way the exoskeleton cannot deliver force in the corresponding direction.
- 3) The lower back interface should be able to rotate freely about the Y-axis. In real overhead works, people may need to horizontally abduct or adduct their arms alongside arm elevation. Enabling free rotation about the Y-axis can make these deviations in movements not constrained by the exoskeleton.
- 4) The lower back interface must not be torque-free except for the Y-axis. Otherwise, the assistive force at the upper arm interface cannot generate any moment around the lower back interface and the force is therefore always in line with the two interfaces. This will compromise the best assistive effect possible.

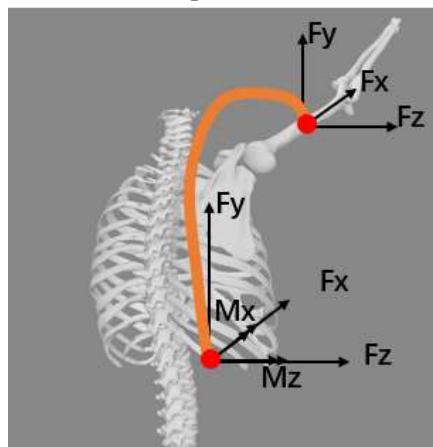


Figure 2.9. The forces and moments that exoskeleton should exert on the user via two interfaces.

2.4. Design Case Study

In conclusion, the upper arm interface must be a ball joint or equivalent and the lower back interface should allow rotation about the Y-direction and constrain all other 5 degrees of freedom. The exoskeleton should provide forces and moments shown in figure 2.9.

2.4.3 Servo-controlled endpoint position

Although free translation in any direction will be constrained, the lower back interface can be moved to different locations by a servo motor for each arm posture and remain still in this posture. With the shape of the compliant beam unchanged, an optimal location for the lower back interface can be found for each arm posture, so that the best assistive effect for each arm posture can be achieved. In this case study, it is explored whether using a servo motor will further improve the assistive effect of the exoskeleton. Servo control and intention detection are beyond the scope.

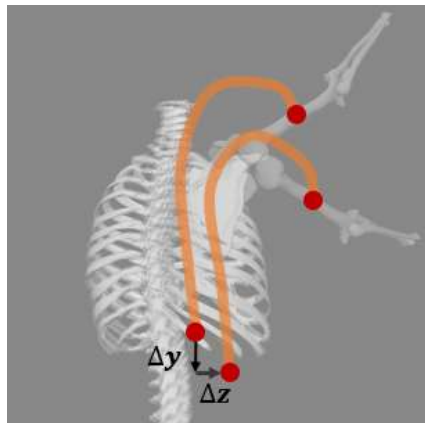


Figure 2.10. The location of the lower back interface can be changed by a servo motor upon arm posture change.

As the lower back interface is supposed to be moved on the lower back by the servo motor, its X-coordinate should not change while seeking for the optimal location, as it is not moving into or away from the lower back, while the movement in Y and Z direction is allowed (see figure 2.10). The interface should neither be moved very close to the centerline of the back, as interference may happen if the user is wearing a pair of exoskeletons.

2.4.4 Working scenarios of the exoskeletons

Different types of work require different features from the exoskeleton, it is possible that compliant beam-based exoskeletons show advantages in assisting some works and show limitations in other works. Therefore, exoskeletons will be designed for two types of work separately, overhead work and full range of motion work. Overhead work only includes arm postures above the horizontal level, and full range of motion work also includes lower arm postures, as shown in figure 2.11. Design results for these two types of work will show how the design tool trades off among the assistive performances in each arm posture.

2.5. Testing designed exoskeletons in the musculoskeletal simulation

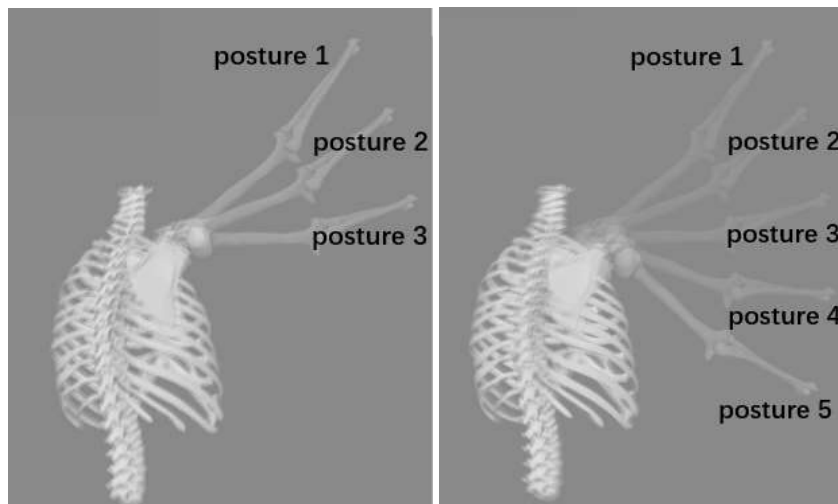


Figure 2.11. Left: arm postures in overhead work. Right: arm postures in full range of motion work.

2.5 Testing designed exoskeletons in the musculoskeletal simulation

2.5.1 Change of activities in individual muscle

The assistive effects of designed exoskeletons will be reflected with changes in muscle activities. The overall performance of an exoskeleton is described by the design objective merged from all design evaluation criteria, while it does not tell any specific effect of the exoskeleton. By looking at the change in each muscle's activity individually, it can be told which muscles are relieved for the most, and which muscles will be compensating in the assisted movement.

2.5.2 Assistive performance of designed exoskeletons on work with loads

To test the versatility of the design tool, designed exoskeletons will be tested to assist work without load and work with 2kg-load in hand in simulated scenarios. As the total muscle activation in loaded work increases, exoskeletons designed for unloaded work may not provide sufficient assistance, and this can be observed if the use of exoskeleton does not result in a higher reduction in muscle activities in loaded work. The simulation of work with 2kg-load in hand is performed with an OpenSim shoulder model with altered hand mass[16].

2.5.3 Robustness of designed exoskeletons under movement perturbations

As compliant beams usually show a strongly position-dependent behavior, the assistive performance of a compliant beam-based exoskeleton may change significantly if the user's motion deviates from the presumed motion used in the optimization procedure. Therefore, a robustness test is done to the designed exoskeletons to see how their assistive performance will change when the user's arm posture is perturbed. Details of this simulated robustness test is in the implementation section in Appendix I section 3.

2.6 Validating the exoskeleton design tool with experiments

2.6.1 Participants

Participants of the experiment include three males with age between 24-29 and height between 168-196 cm. Female participants were not recruited due to the possible inconvenience in the measurement of EMG in pectoralis major. All participants signed the Informed Consent and reported good health and no ongoing shoulder musculoskeletal disorders. The HREC of this experiment is approved by TU Delft.

2.6.2 Experiment setups

As the scope of this project is to develop and validate the exoskeleton design tool, exoskeletons designed in the case study will not be prototyped. The effect of a selected exoskeleton on the human body will be tested by

2.6. Validating the exoskeleton design tool with experiments

creating equivalent assistive forces at each arm postures considered in the design procedure. The experiment aims to test if the assistive forces from the selected exoskeleton will cause changes in muscle activities on the participants that are similar to the changes in muscle activities predicted by the test in the musculoskeletal simulation.

The exoskeleton-equivalent forces are created with a weight-and-pulley system (figure 2.12). The magnitude of the force is controlled by the mass of a counterweight, which is calculated by $mass = F/(9.8N/kg)$ and rounded with a resolution of 0.1 kg. The direction of force is controlled by the orientation of the cable connecting the counterweight and the arm cuff. To test the robustness of the exoskeleton at the same time, the orientation is not measured with any instrument, it is estimated with reference to the participant's arm posture by eyes instead.

To replicate the “moment free” property of the upper arm interface, the arm cuff is designed as shown in figure 2.13. As the rope connecting the arm cuff and the cable can rotate freely around the arm, there is no moment generated about the central axis of the upper arm. Also, only force can be transmitted to the arm cuff due to the usage of cable and rope.

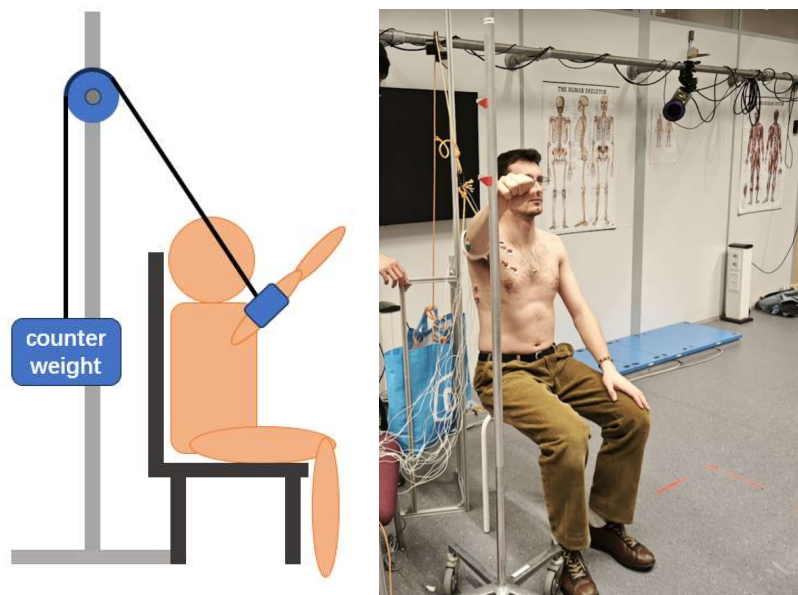


Figure 2.12. Left: schematic sketch of the experiment setup. Right: experiment setup in practice.

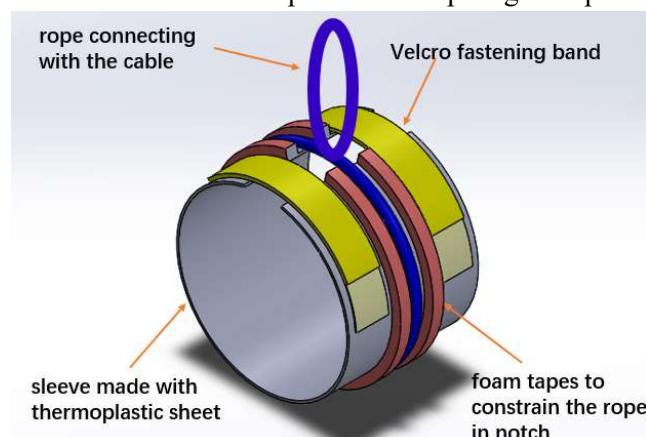


Figure 2.13. Design of the arm cuff.

2.6.3 Measurement of muscle activities

2.6. Validating the exoskeleton design tool with experiments

Musculoskeletal simulation shows that designed exoskeletons will change the activities in trapezius, serratus anterior, deltoid anterior, deltoid medial, latissimus dorsi, pectoralis major, infraspinatus, pectoralis minor, and bicep short head(will be shown in section 3.2). However, it is not practically possible to measure the activities in infraspinatus and pectoralis minor with surface EMG, and wearing the arm cuff will also cover the location of EMG electrodes on biceps. As a result, activities in the rest muscles were measured. surface EMG measurement was conducted according to the SENIAM guidelines[19], and the electrode attachments are shown in figure 2.12. The experiment used a bipolar EMG measurement unit from TMSi.

In the experiment, each participant was asked to keep their right arms to the position around the three selected postures in the design procedure(as shown in figure 2.11 left). In each posture, 6 trials of EMG measurement were collected, each lasting for at least 10 seconds. 3 trials are with the exoskeleton-equivalent force applied to the participant as EXO test groups, and the other 3 trials are noEXO control groups without external forces applied. Trials of test groups and control groups were done in turns to prevent muscle activities falling into specific patterns, and a rest was arranged between trials.



Figure 2.14. EMG electrodes attachment.

2.6.4 Experiment procedure

Each participant went through the following procedure in the experiment.

- 1) Shave the attachment locations of EMG electrodes and clean with alcohol pads, attach electrodes on relevant muscles as figure 2.14, and perform a set of movements to record maximum voluntary contraction (MVC).
- 2) The participant sits on a chair, elevates right arm to a position around the first arm posture. The researcher records a trial (about 10 sec) of EMG data for the noEXO control group and marks participant's hand location on the bar besides. The participant puts down arm and relaxes.
- 3) The researcher adjusts the counterweight to required mass and connects the cable to the arm cuff. The participant elevates arm to the posture where his hand reaches the mark on the bar besides. The researcher records a trial of EMG data for the EXO test group when the participant's arm is stable. The participant puts down arm and relaxes. The researcher disconnects the cable and the arm cuff.
- 4) Repeat step 2) and 3) to record two more trials each for noEXO and EXO group with same arm posture.
- 5) Repeat step 2), 3), and 4) for the other two arm postures.

With each participant, $3 \text{ trials/group/posture} \times 2 \text{ groups} \times 3 \text{ postures} = 18 \text{ trials}$ EMG data was recorded.

2.6.5 Data processing

The EMG data was processed with a custom code written in MatLab filtering the raw EMG data with a bandwidth of 20-400Hz, rectifying, smoothing with a window of 300ms, and normalizing to the MVC of each muscle[20]. The first two seconds in each trial of EMG data were excluded from processing, as muscle activities take time to reach equilibrium. The processed EMG data of each participant were treated individually, with the three trials of the same group(test or control) of each arm posture combined together. The distribution of these combined EMG data was checked per participant per muscle by Lilliefors test, and the median of each muscle's activity per group per arm posture was computed, as the distribution was not normal. The variance was also

2.6. Validating the exoskeleton design tool with experiments

calculated. Differences of activities in each muscle between EXO(test) and noEXO(control) groups were calculated with medians of muscle activities. Differences in muscle activities between EXO and noEXO(control) group will show if the resultant of the exoskeleton design tool can reduce activities in major actuating muscles of arm elevation, and it can also suggest the robustness of the designed exoskeleton as the participants motions are not strictly same as the motion file used in design procedure.

A statistical analysis was performed to evaluate the effectiveness of the selected exoskeleton design. Considering the independent variable only has two levels, EXO and noEXO, and data were not normally distributed, Wilcoxon signed rank test was used to examine the difference between EXO and noEXO groups per participant per muscle. The null hypothesis tested was “the difference between the median activities of a muscle in EXO and noEXO group is not equal to the difference between the median values of this muscle’s EMG data in EXO and noEXO group”.

3

Results

3.1 Performance of designed exoskeletons

As specified in previous sections, two types of optimization objectives and two types of lower-back interface were used to optimize for exoskeletons assisting two working scenarios, resulting in six final designs described in table 3.1. The performances of resulting exoskeleton designs are summarized in table 3.2. Normalized total muscle activation is the fraction between the total muscle activation with the exoskeleton and without the exoskeleton. Normalized joint reaction force is the fraction between the magnitude of joint reaction force in the glenohumeral joint with the exoskeleton and without the exoskeleton. Maximum muscle activity is presented with the muscle in which the maximum activity occurs with the exoskeleton. Maximum muscle compensation is that in the muscle presented the difference between its activities with and without the exoskeleton is the largest among all muscles. Force fraction along the upper arm is pointing to the elbow for positive values, and pointing to the shoulder for negative values. Design 2 and design 5 were selected for simulated tests, and their geometry with changing arm postures are shown in figure 3.1 and 3.2. Design 2 was selected for the experimental test.

Table 3.1. Description of each design. Dimensions of the compliant beam part is in Appendix II.

Design	Minimize friction in upper arm interface	Servo motor-controlled lower back endpoint position	Assisted type of work
1	no	no	Overhead work
2	yes	no	Overhead work
3	no	yes	Overhead work
4	no	no	Full range of motion
5	yes	no	Full range of motion
6	no	yes	Full range of motion

Table 3.2. Main performances of the designs. SA-serratus anterior, DA deltoid anterior, PMT-pectoralis major thorax, TS-trapezius scapula, PMin-pectoralis minor, IS-infraspinatus, subscript “s”, “m”, and “i” refer to superior, medial, and inferior respectively.

Design	Arm posture	Normalized total muscle activation	Normalized joint reaction force	Maximum muscle activity /%MVC	Maximum muscle compensation /%MVC	force fraction along upper arm /N
1	1	0.52	0.76	SAm 8.8	TSi 0.94	14.38
	2	0.39	0.62	DA 5.35	PMin 3.46	16.43
	3	0.47	0.45	PMTi 8.03	PMTi 8.03	7.48

3.1. Performance of designed exoskeletons

2	1	0.57	0.79	SAm 11.93	SAs 0.98	0.87
	2	0.41	0.65	DA 5.50	PMTi 3.44	3.32
	3	0.42	0.48	PMTi 7.15	PMTi 7.15	0
3	1	0.37	0.64	ISi 6.10	PMTi 3.23	29.26
	2	0.39	0.61	DA 5.58	PMin 3.31	23.59
	3	0.35	0.53	DA 4.77	PMTi 3.32	6.78
4	1	0.77	0.89	SAm 15.61	TSi 0.04	4.46
	2	0.62	0.80	SAm 9.22	TSi 1.02	5.76
	3	0.47	0.68	DA 7.38	PMTi 2.54	2.62
	4	0.39	0.56	DA 4.40	PMTi 3.25	-5.92
	5	0.69	0.74	PMTi 8.07	PMTi 8.07	-25.44
5	1	0.77	0.89	SAm 15.76	SAs 0	2.92
	2	0.62	0.81	SAm 9.43	TSi 0.63	3.28
	3	0.48	0.67	DA 7.46	PMTi 2.48	0.93
	4	0.39	0.57	DA 4.55	PMTi 2.94	-4.07
	5	0.66	0.73	PMTi 7.22	PMTi 7.22	-16.48
6	1	0.75	0.86	SAm 13.49	TSi 4.63	26.45
	2	0.41	0.66	DA 6.16	PMTi 2.52	8.92
	3	0.35	0.54	DA 4.87	PMTi 3.28	4.59
	4	0.35	0.52	TSi 4.43	TSi 4.43	7.40
	5	0.52	0.71	PMTi 5.43	PMTi 5.43	-27.42

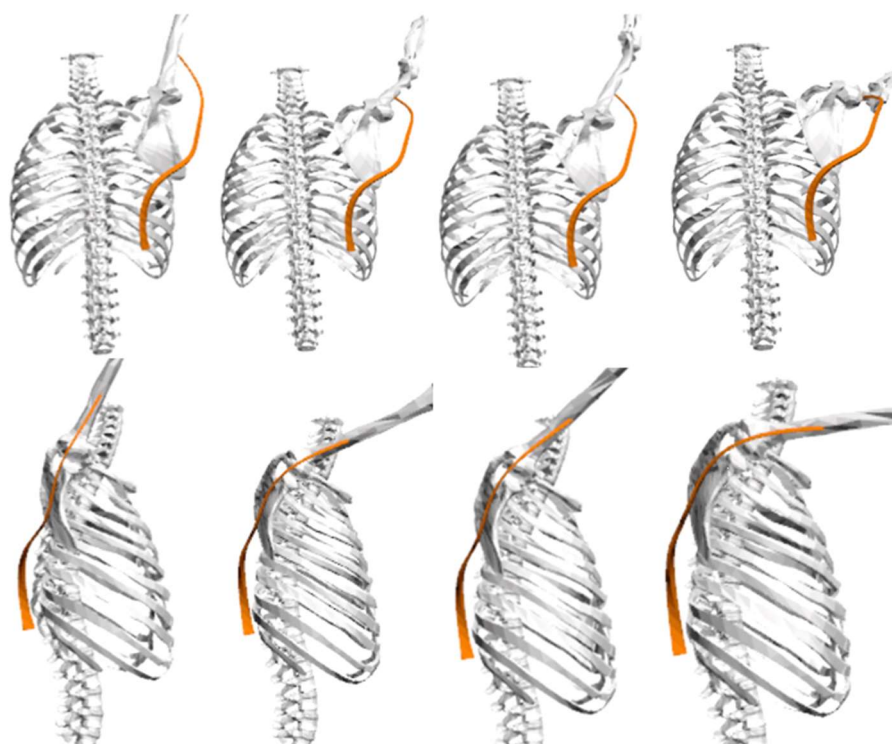


Figure 3.1. Exoskeleton design 2 on musculoskeletal model in initial posture and arm posture 1-3

3.2. Changes in muscle activities with designed exoskeletons

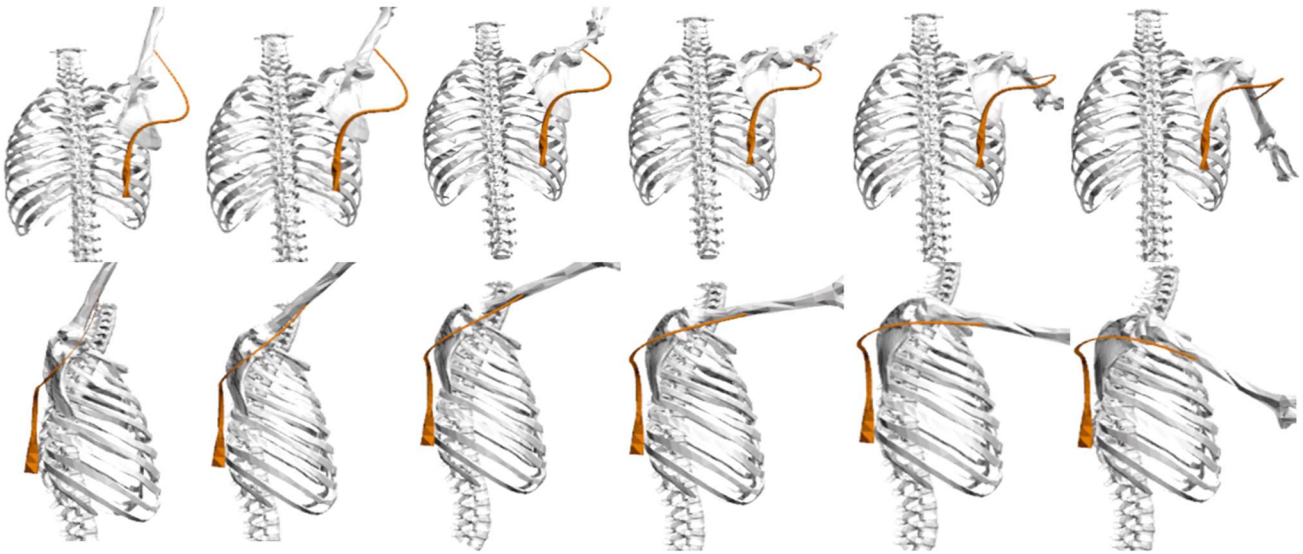
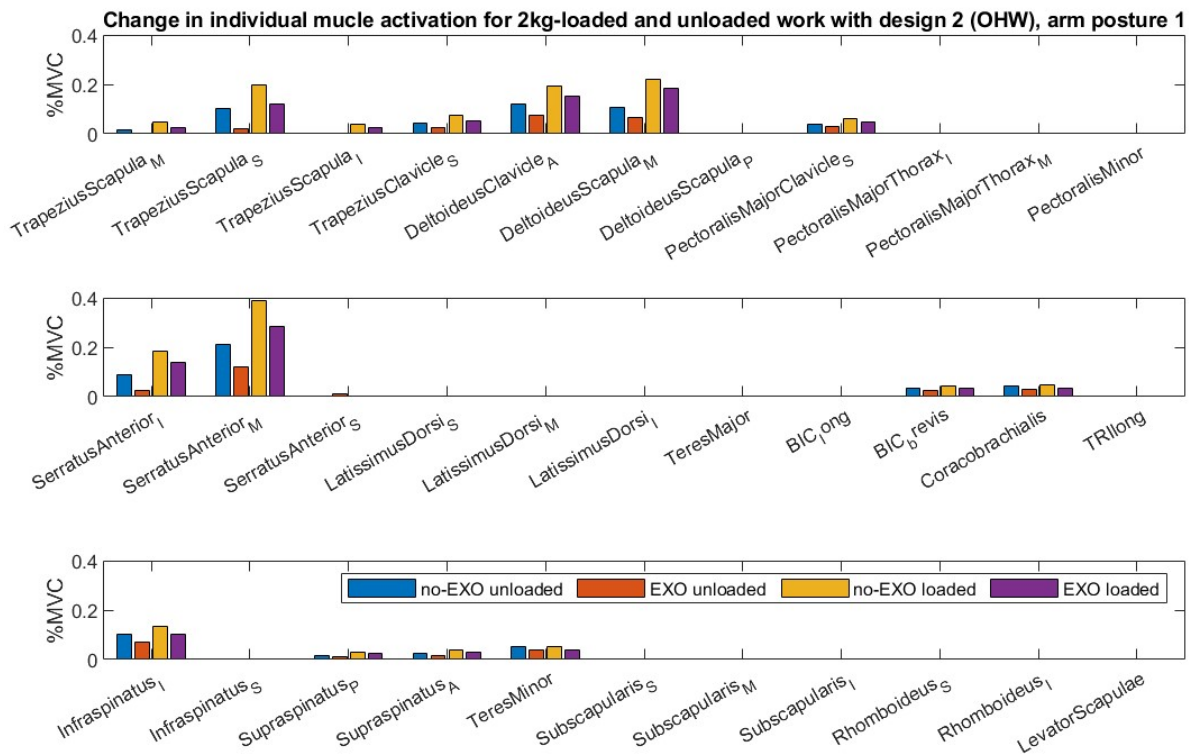


Figure 3.2. Exoskeleton design 5 on musculoskeletal model in initial posture and arm posture 1-5

3.2 Change in muscle activities with designed exoskeletons, 2kg-loaded and unloaded tasks

By modeling movements assisted with the exoskeleton design 2 and 5, activities in each muscle were computed. Activities in all 33 muscles in the OpenSim musculoskeletal model are shown in figure 3.3 and 3.4. The muscles are presented in an order from bigger muscles to smaller muscles, from primary shoulder flexors to shoulder extensors, and lastly stabilizers of the shoulder. For design 2, overhead arm postures were modeled, and all five arm postures were modeled for design 5. It should be noted here that the musculoskeletal simulation tends to underestimate muscle activities, which will be explained in section 4.2, so the focus should be in the reduction in muscle activities with the exoskeleton.



(a)

3.2. Changes in muscle activities with designed exoskeletons

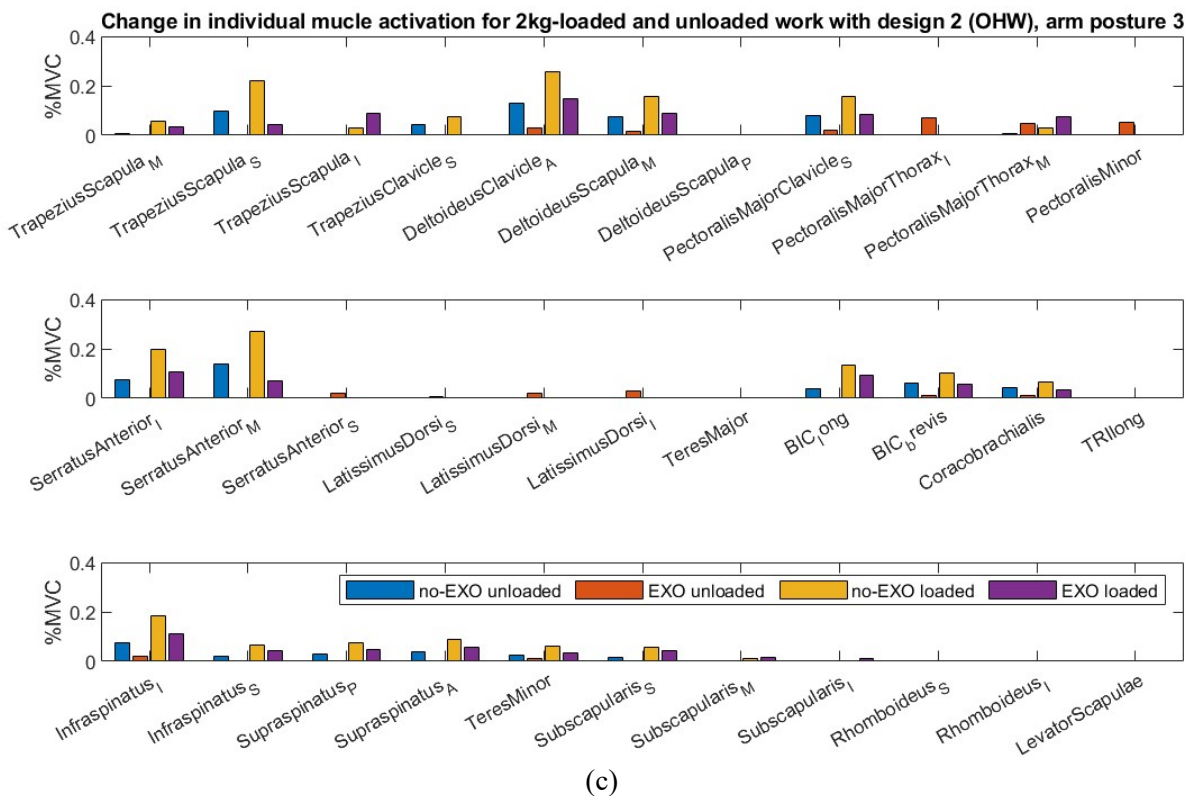
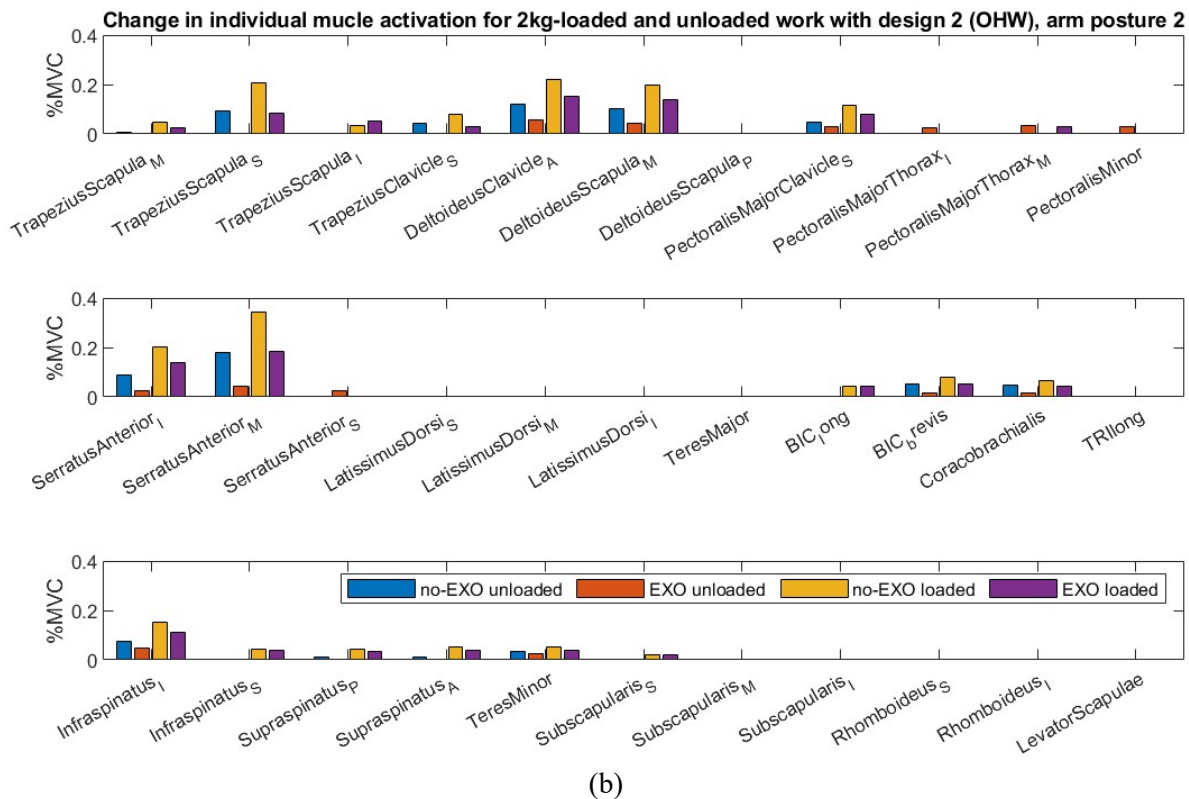
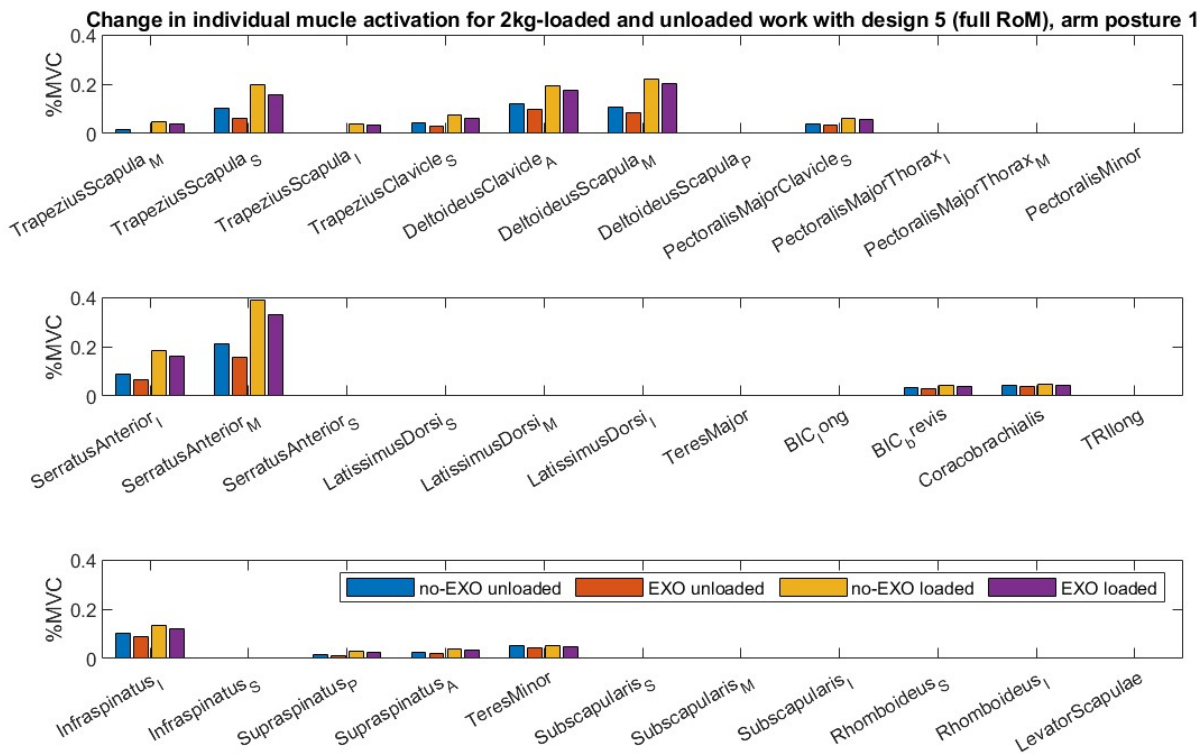
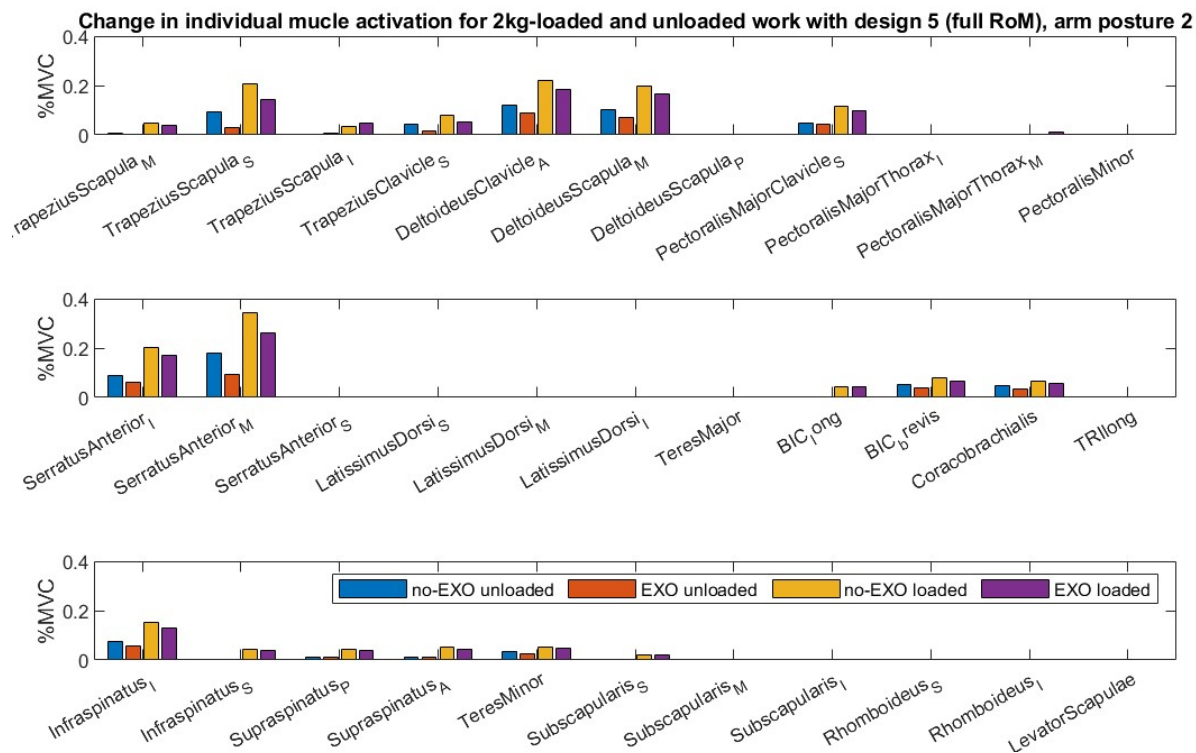


Figure 3.3 (a-c). Muscle activities in arm posture 1-3 with and without the exoskeleton design 2.

3.2. Changes in muscle activities with designed exoskeletons

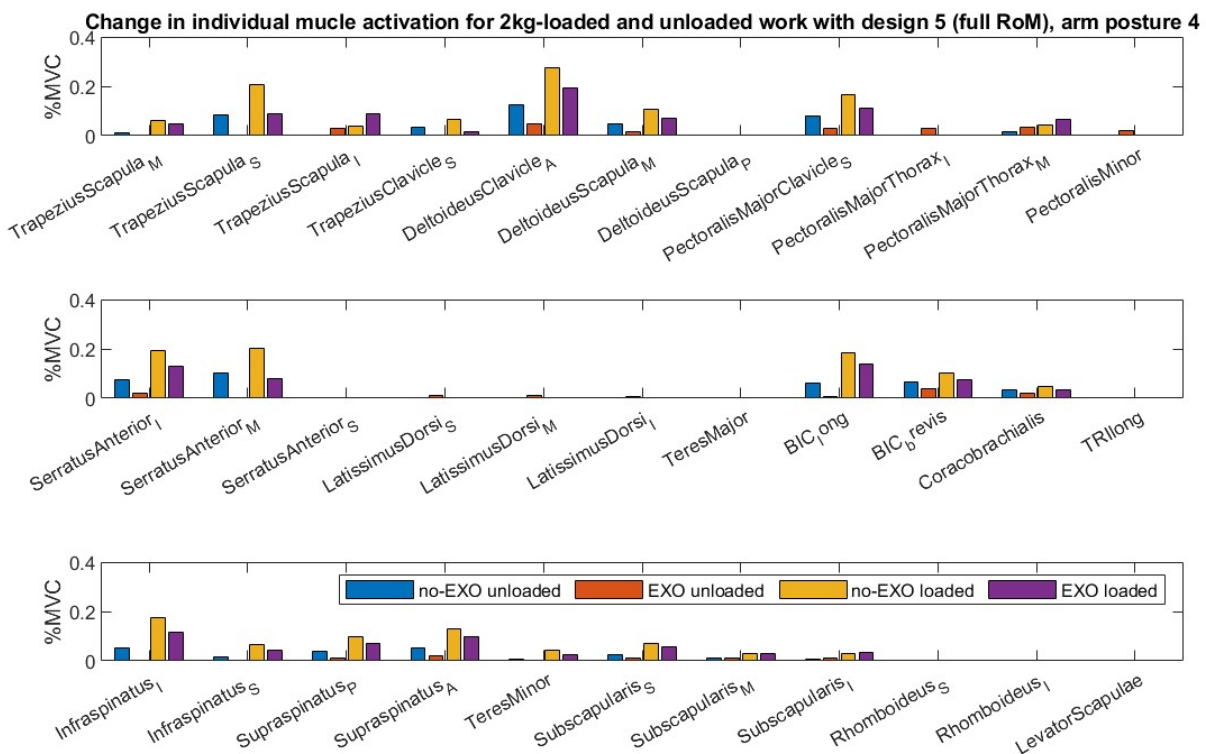
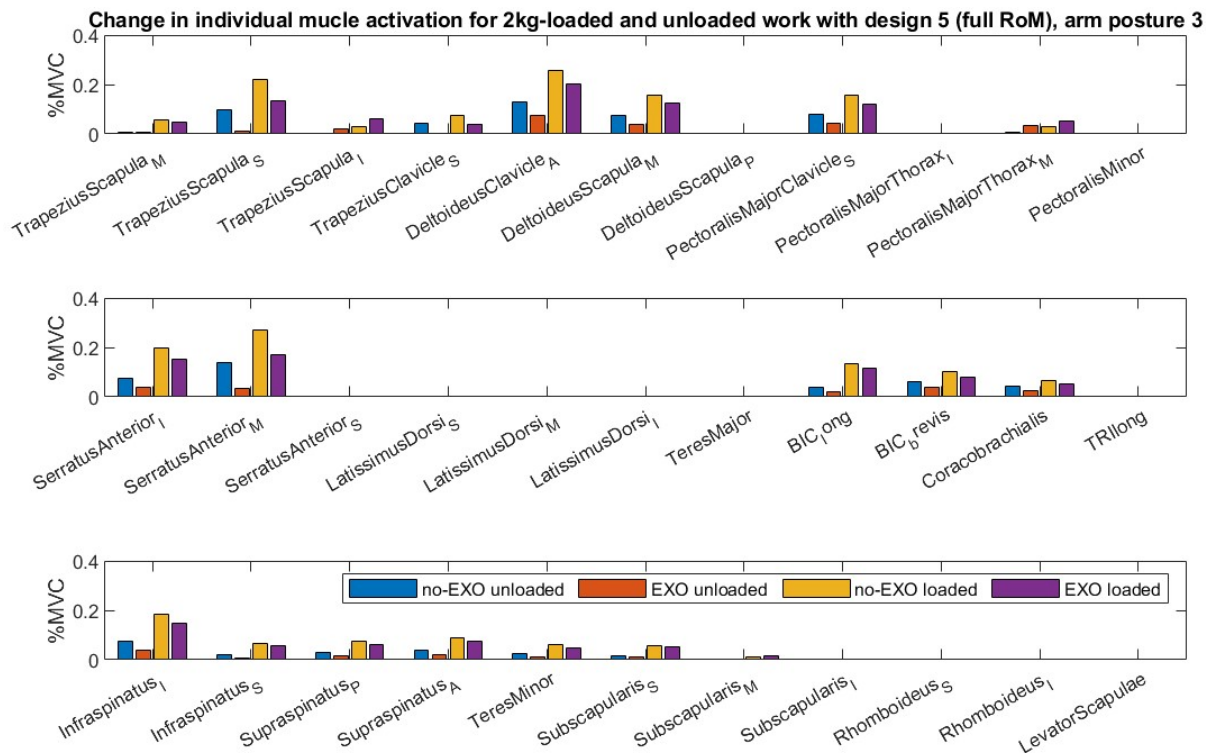


(a)



(b)

3.2. Changes in muscle activities with designed exoskeletons



3.3. Robustness of the design

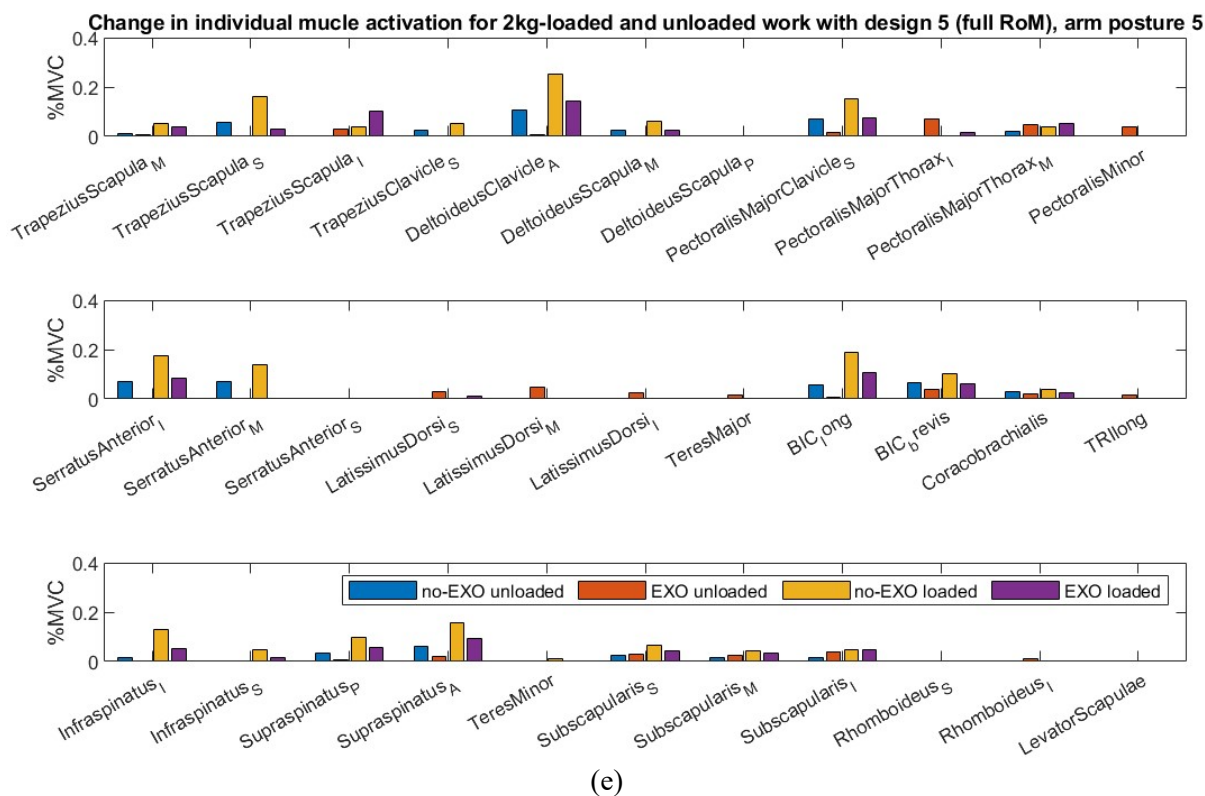


Figure 3.4 (a-e). Muscle activities in arm posture 1-5 with and without the exoskeleton design 5.

3.3 Robustness of the design

The performance of the exoskeleton design 2 and 5 is represented with color scales, with the range of perturbation span the square area defined by its X and Y axes. Similarly, only overhead arm postures were simulated for design 2 and all five arm postures were simulated for design 5. In most perturbed motions, the assistive performance of two exoskeletons may become slightly poorer than in the unperturbed motion, but the assistive effect is still positive. Only in arm posture 5, the assistive effect of the exoskeleton design 5 becomes negative in a small range.

3.3. Robustness of the design

Change of total muscle activation and joint reaction force with perturbation to arm posture, design 2(OHW)

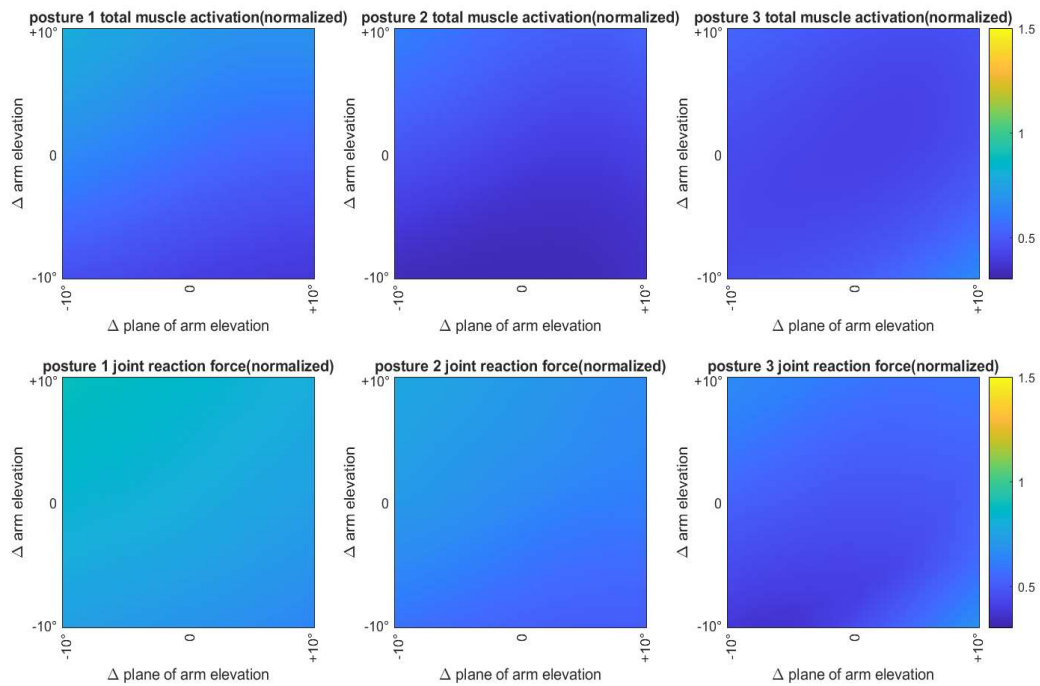


Figure 3.5. Change of total muscle activation with motion perturbation, design 2, arm posture 1-3

Change of total muscle activation and joint reaction force with perturbation to arm posture, design 5(full RoM)

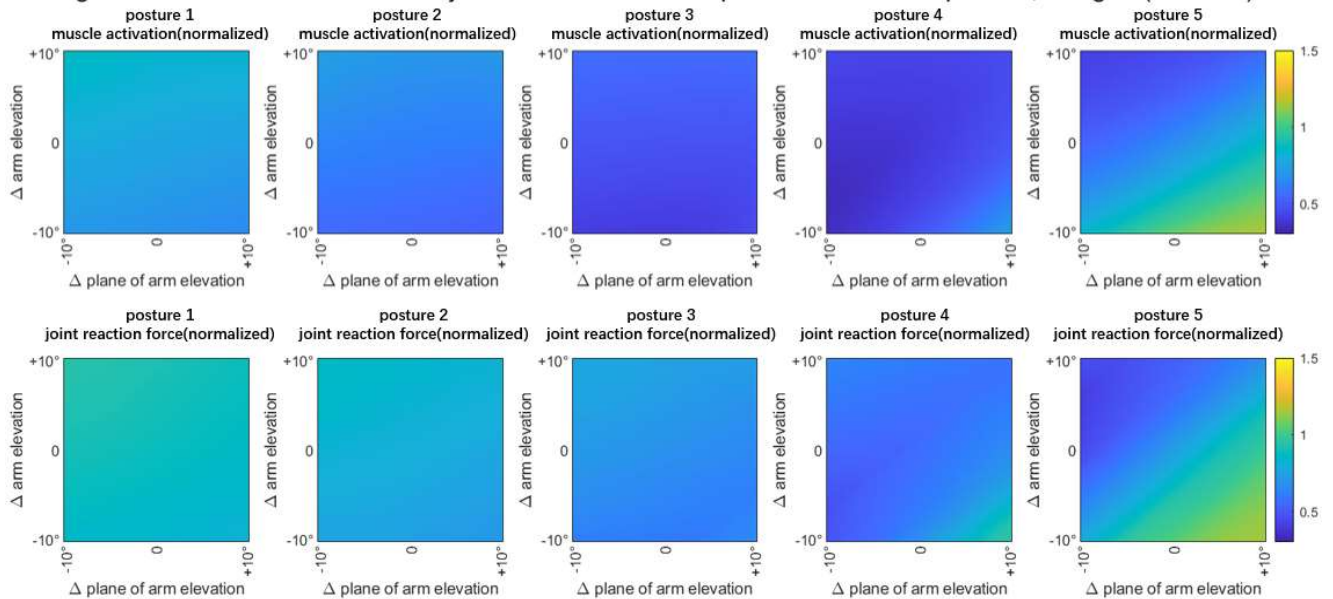
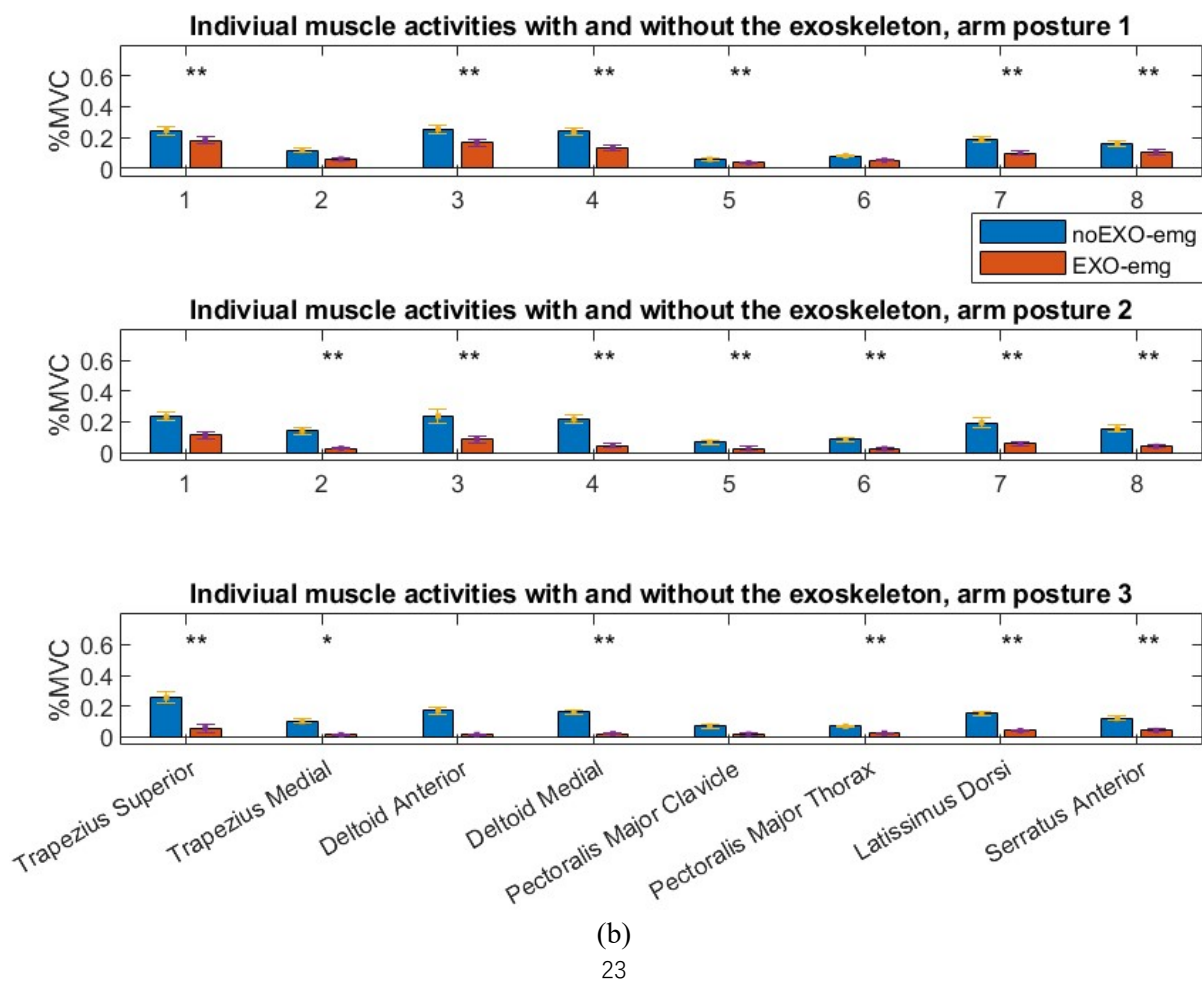
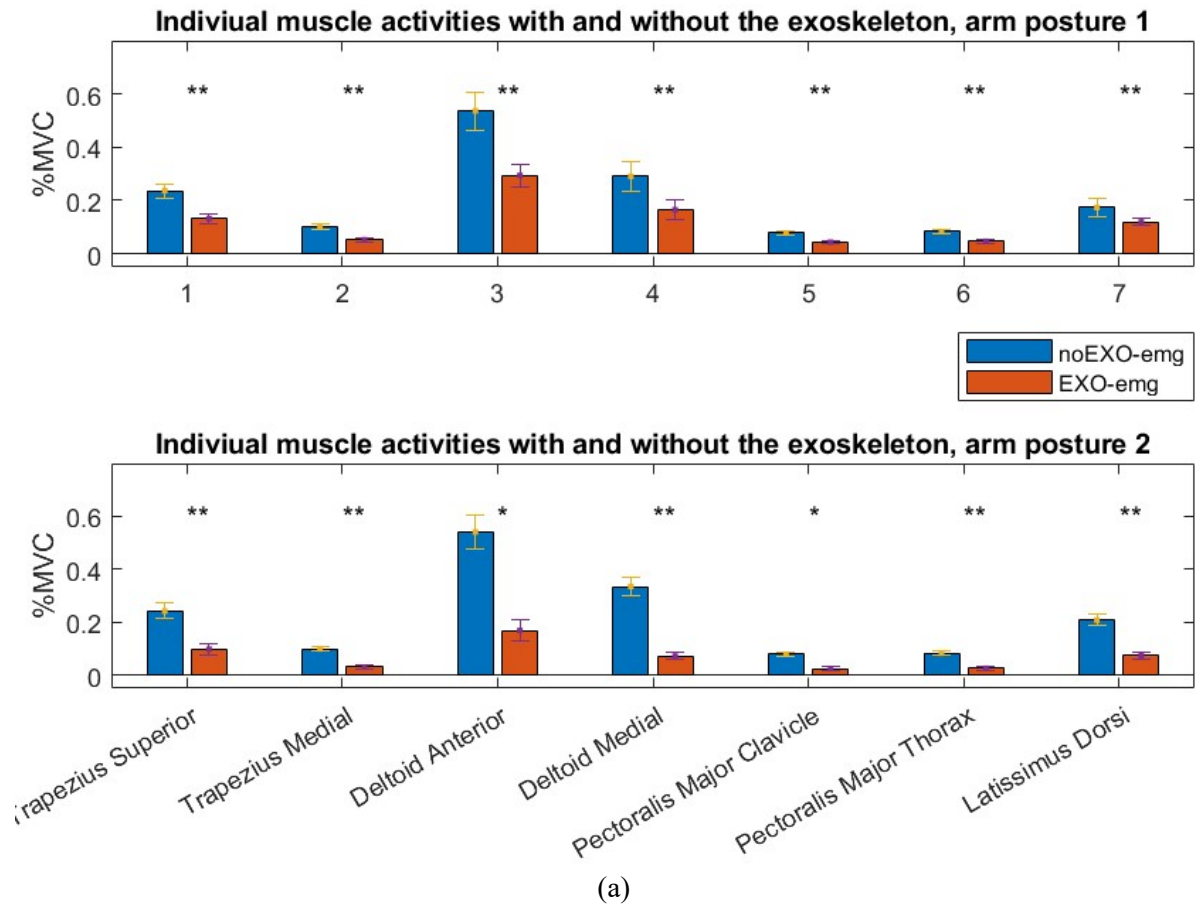


Figure 3.6. Change of total muscle activation with motion perturbation, design 5, arm posture 1-5

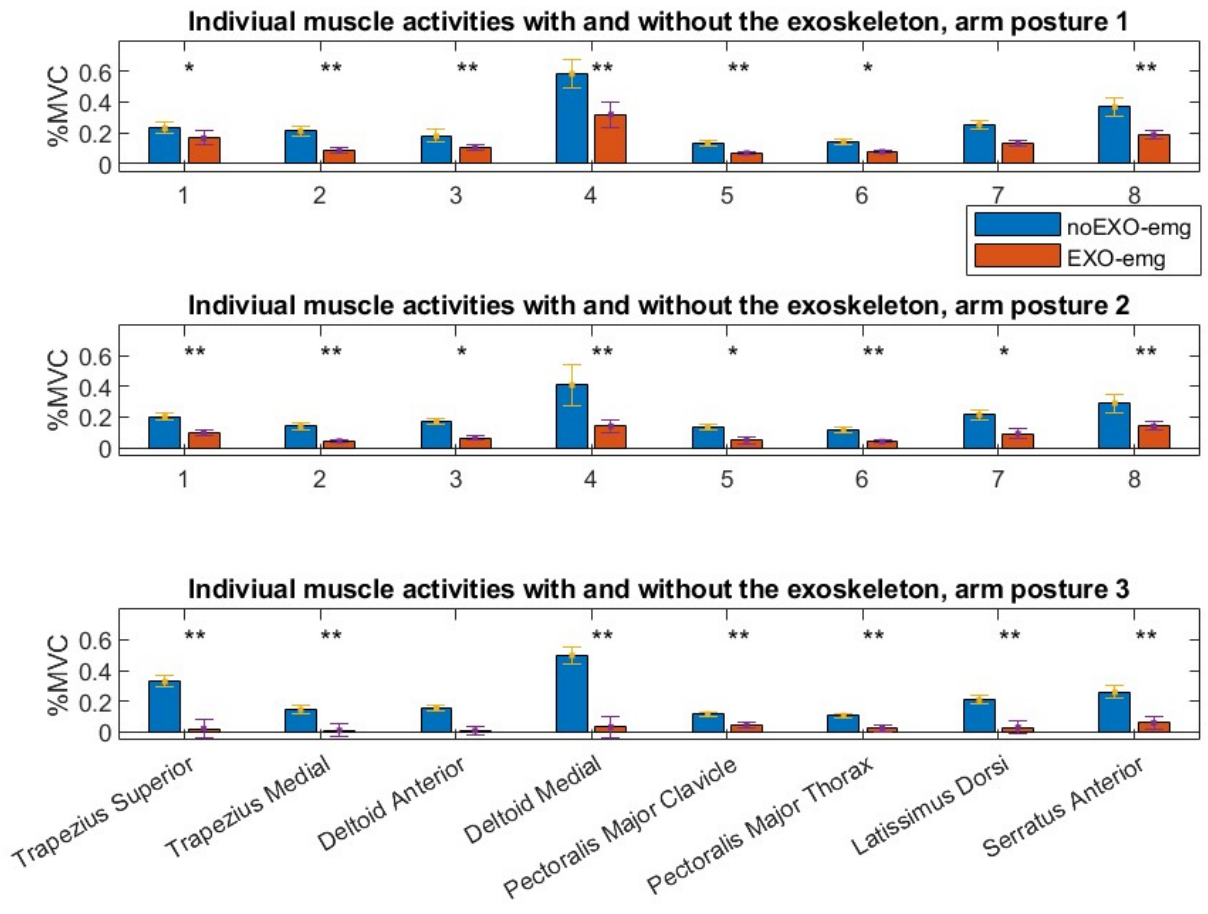
3.4 Experiment Results

The median and variance of muscle activities in each measured muscle of each participant in posture 1-3 with and without exoskeleton-equivalent forces of design 2 are shown in figure 3.7. Median of EMG is used to represent the average level of muscle activities, and the error bar is the standard deviation. **- $p < 0.001$ for the null hypothesis, *- $0.001 < p < 0.05$ for the null hypothesis. For participant 1, arm posture 3 was not performed, and surface EMG was not measured in serratus anterior.

3.4. Experiment results



3.4. Experiment results



(c)

Figure 3.7 (a-c). Muscle activities of participants 1-3 with and without the exoskeleton-equivalent forces from design 2 of arm posture 1-3.

4

Discussion

4.1 Performance of design results

4.1.1 Overall performance of different design concepts

From table 2 it can be seen that this new exoskeleton design tool found a range of designs based on compliant beams that significantly reduce the total muscle activation in different ranges of arm elevated works without inducing negative biomechanical effects like excessive muscle compensation or large joint reaction forces in the glenohumeral joint. When the assisted range of motion increases, comparing design 1 and 4, 2 and 5, the design tool cannot find a solution that provides optimal assistance in all arm postures, it compromises among the assistive performance in each arm posture to reach an overall good assistive performance. Comparing design 1 and 2, and 4 and 5, it is possible to minimize the force fraction along the humerus in the upper arm interface without significantly compromising other performances. Comparing design 1 and 3, and 4 and 6, using a servo motor to change the location of the lower back interface with arm postures slightly increases the assistance, while it should be considered if the effect is significant enough to justify the added cost, weight, and volume of a servo motor.

4.1.2 Change in individual muscle activities

Figure 3.3 and 3.4 show how the reduction in total muscle activities is shared by each muscle. Reduced activities occur in most muscles that are activated for the motion. Most significant reductions occur in trapezius, deltoids, and serratus anterior, which are the main contributing muscles of arm elevation. When the arm is in lower postures (arm posture 3-5) and the assistive force from the exoskeleton is larger, slight compensation occurs in muscles contributing to scapula depression and humerus extension.

4.1.3 Versatility of the exoskeleton

Comparing the assistive effects in unloaded task and 2kg-loaded task, design 2 and 5 show moderate versatility in assisting arm elevated work with small loads. When there is a 2kg-load in hand, the exoskeletons can still significantly reduce muscle activities, and sometimes by a higher level compared to the unloaded case. Compensation in muscles is also reduced, as the load in hand to some extent counter-balanced the excessively high assistive force from the exoskeletons. However, muscle activities in the loaded task still have space for further reduction, so it is reasonable to doubt that these exoskeletons cannot provide sufficient assistance when the load gets larger.

4.1.4 Robustness of the exoskeleton

Figure 3.5 and 3.6 show design 2 and 5 have good robustness when arm postures are perturbed from the “standard” posture considered in the design procedure. Horizontal abduction and adduction of the arm do not impose noticeable change to the assistive effects of exoskeletons. Changing the flexion level of the arm also barely changes the assistive effects, except in arm posture 5. In arm posture 5, the assistive force is already excessively large, and compensation already occurs in some muscles(see figure 3.4-e). Putting the arm lower will increase the deformation in the exoskeleton and results in an even larger assistive force and further increases

4. Discussion

muscle compensation, and thus decreases the overall assistive effect of the exoskeleton.

4.2 Difference between predicted change in muscle activities and EMG results

As shown in figure 3.7, significant reduction of muscle activities can be observed in trapezius (more in the upper part), deltoids, and serratus anterior, which is similar to the results of musculoskeletal simulation. The similarity between the simulation and experiment also suggests coherence to the good robustness of the exoskeleton predicted in the simulated robustness test. Although participants' arm posture more or less deviated from the "standard" arm postures used in design procedure, assistive forces from the exoskeleton still showed very good assistive effects.

The major difference between the results of experiment and simulation is that muscle compensation was not observed in latissimus dorsi or pectoralis major in participants. There are a few possible explanations for this.

- 1) The musculoskeletal modeling of the shoulder is not a complete copy of real biomechanics in OpenSim. For example, muscle paths may deviate from the real situation in the human body and moment arms of muscles therefore change. Also, OpenSim isolates the shoulder area from the rest of the body and therefore does not include some interaction between the shoulder and the rest of the body, and shoulder muscles thus have fewer forces and moments to balance off.
- 2) OpenSim and the RMR solver have a tendency to underestimate muscle activities, because co-contraction of muscles is not considered in the computation of muscle activities. Co-contraction of muscles will increase activities in both agonists and antagonists.
- 3) The OpenSim shoulder model used in the design procedure is smaller than an average male, so an external force causing muscle compensation in the shoulder model may not cause muscle compensation in the selected participants. However, this explanation was excluded after performing simulation with a scaled-up shoulder model, details shown in Appendix III.

4.3 Further validation of the design tool

Although high coherence is shown in the predicted muscle activities by the musculoskeletal simulation and from the experiment, this new exoskeleton design tool needs to be further validated for a few aspects.

- 1) The predicted activities in deeper muscles, like the rotator cuffs, are not verified in the experiment as their activities cannot be measured with surface EMG. Different techniques should be used to collect the activities in deeper muscles to verify all predicted changes in muscle activities by the musculoskeletal simulation.
- 2) It should be verified if reaction forces in the glenohumeral joint are not increased with the use of exoskeletons as predicted by the design tool. To do this, a similar experiment can be done under magnetic resonance imaging to record the change of the glenohumeral joint space during the use of designed exoskeletons.
- 3) A questionnaire should be used to record participants' perceived fatigue level during arm elevation with and without designed exoskeletons. It should be verified that a reduction in total muscle activation predicted by the design tool is correlated with reduced fatigue level in real working scenarios.
- 4) A prototype of the designed exoskeleton should be fabricated. Participants should wear the exoskeleton to evaluate it in movements. Also, regular methods to evaluate an exoskeleton can be applied in this case.

4.4 Limitation of the design tool and recommendation on future development

The design tool currently has two major limitations. First, all design criteria and some nonlinear constraints are merged to one objective function, resulting in poor transparency and controllability in optimization. An optimizer that can handle multiple nonlinear constraints and objective functions needs to be found for this design tool. Second, design criteria of this design tool are not well supported by understandings of shoulder biomechanics. For example, it is not clear which level of muscle activity can cause chronic muscle pain, or

4. Discussion

which level of reaction force in the glenohumeral joint will trigger cartilage damage. Currently, all reasoning to the selection of design criteria is based on previous results of musculoskeletal simulations or a general understanding of shoulder disorders, and this does not promote reliability of the design tool at all. This limitation is not expected to be solved in recent years, as it completely relies on the development in the understanding of shoulder biomechanics.

For future development, the first recommendation would be to establish a procedure to test the prototype of the resultant designs on human subjects, as this is the only way to formally validate this design tool. Proper yet affordable techniques should be selected to fabricate the prototype. As it is not always possible to measure the surface EMG of all shoulder muscles, it should be found which muscles are measurable and can reflect the assistive effect of the prototype. Motion tracking can also be used during the experiment to observe how motion patterns change with the use of the prototype.

Another recommendation is to add the scaling of the OpenSim musculoskeletal model to the design tool to better represent the size of target users of the exoskeleton to be designed. As compliant beam-based exoskeletons will mostly be fabricated by 3D printing, this measure can strongly enhance the design tool's capability in designing customized exoskeletons. Lastly, it should be considered that previous studies on shoulder exoskeletons reported shoulder kinematics changed with the use of exoskeletons[5, 12]. This design tool should also be featured with predictive simulation to anticipate how the designed exoskeleton will change the motion pattern of the user. Corresponding criteria to evaluate if the change in motion pattern will cause negative effects on users' musculoskeletal wellness.

5

Conclusion

In this project a new design tool for shoulder exoskeleton was developed, and several designs with different interface mechanisms and using scenarios were generated to validate the design tool. The design tool has two main advances, it can predict the biomechanical effects of an exoskeleton with musculoskeletal simulation in the design procedure, as well as iteratively optimize the assistive performance of the exoskeleton. This design tool enables “human-in-the-loop” design of shoulder exoskeletons, which contributes to the understanding of how exoskeletons change shoulder biomechanics, and it will also greatly save financial and time investment in the development of exoskeletons.

The design tool was validated by the musculoskeletal simulation OpenSim and an experiment on human subjects testing the effectiveness of a selected exoskeleton design on reducing muscle activities. OpenSim simulation showed that the selected exoskeleton design could significantly reduce activities in most muscles and will not impose any negative effects on shoulder biomechanics. Simulation also suggested the selected exoskeleton design had good versatility in assisting works with different loads in hand and good robustness under perturbed arm postures. In the experiment, significant reduction can be observed in the activities of trapezius, latissimus dorsi, deltoids, pectoralis, and serratus anterior. The predicted robustness of the exoskeleton was also supported by the fact that the assistive effect of the exoskeleton was significant despite arm postures of participants deviating from standard postures.

Suggestions on future development mainly focus on further validation of the design tool and supporting the design criteria with more biomechanical knowledge. A prototype of the resultant design should be fabricated with proper methods, so that it can be validated directly. The design tool’s prediction on shoulder biomechanics should be verified with experiments recording activities in more muscles, and the prediction on reaction forces in the glenohumeral joint, which reflects the change in joint space, should be verified under medical imaging if there is any chance. Biomechanical knowledge about the trigger and prevention of shoulder musculoskeletal disorders should be better developed and expressed in a more quantified manner, in order to better reason the choices on exoskeleton design criteria. It is especially crucial to identify the relation between muscle activity level and chronic muscle pain, and the relation between glenohumeral joint reaction force and shoulder impingement syndrome.

References

- [1] P. V. Jan de Kok, Jacqueline Snijders, Georgios Roullis, Martin Clarke, and P. v. D. Kees Peereboom, Iñigo Isusi, "Work-related musculoskeletal disorders : prevalence, costs and demographics in the EU," 2019.
- [2] Ottobock Corporation. (01.05). *iX Shoulder AIR Exoskeleton*. Available: <https://www.suitx.com/en/products/ix-shoulder-air-exoskeleton>
- [3] COMAU. (01.05). *MATE XT*. Available: <https://mate.comau.com/mate-xt/>
- [4] M. Tschiersky, E. E. G. Hekman, J. L. Herder, and D. M. Brouwer, "Gravity Balancing Flexure Spring Mechanisms for Shoulder Support in Assistive Orthoses," *IEEE Transactions on Medical Robotics and Bionics*, Article vol. 4, no. 2, pp. 448-459, 2022.
- [5] D. J. Hyun, K. Bae, K. Kim, S. Nam, and D. H. Lee, "A light-weight passive upper arm assistive exoskeleton based on multi-linkage spring-energy dissipation mechanism for overhead tasks," *Robotics and Autonomous Systems*, Article vol. 122, 2019, Art. no. 103309.
- [6] K. Desbrosses, M. Schwartz, and J. Theurel, "Evaluation of two upper-limb exoskeletons during overhead work: influence of exoskeleton design and load on muscular adaptations and balance regulation," *European Journal of Applied Physiology*, Article vol. 121, no. 10, pp. 2811-2823, 2021.
- [7] S. Alabdulkarim and M. A. Nussbaum, "Influences of different exoskeleton designs and tool mass on physical demands and performance in a simulated overhead drilling task," *Applied Ergonomics*, Article vol. 74, pp. 55-66, 2019.
- [8] A. Day, N. F. Taylor, and R. A. Green, "The stabilizing role of the rotator cuff at the shoulder - Responses to external perturbations," *Clinical Biomechanics*, Article vol. 27, no. 6, pp. 551-556, 2012.
- [9] S. De Bock *et al.*, "Passive shoulder exoskeleton support partially mitigates fatigue-induced effects in overhead work," *Applied Ergonomics*, Article vol. 106, 2023, Art. no. 103903.
- [10] A. Seth *et al.*, "OpenSim: Simulating musculoskeletal dynamics and neuromuscular control to study human and animal movement," *PLoS Computational Biology*, Article vol. 14, no. 7, 2018, Art. no. e1006223.
- [11] J. Rasmussen, "Chapter 8 - The AnyBody Modeling System," in *DHM and Posturography*, G. P. Sofia Scataglini, Ed.: Academic Press, 2019, pp. 85-96.
- [12] A. van der Have, M. Rossini, C. Rodriguez-Guerrero, S. Van Rossom, and I. Jonkers, "The Exo4Work shoulder exoskeleton effectively reduces muscle and joint loading during simulated occupational tasks above shoulder height," *Applied Ergonomics*, Article vol. 103, 2022, Art. no. 103800.
- [13] J. C. Gillette, S. Saadat, and T. Butler, "Electromyography-based fatigue assessment of an upper body exoskeleton during automotive assembly," *Wearable Technologies*, Article vol. 3, 2022, Art. no. e23.
- [14] B. Italo *et al.*, "Does enforcing glenohumeral joint stability matter? A new rapid muscle redundancy solver highlights the importance of non-superficial shoulder muscles," *bioRxiv*, p. 2023.07.11.548542, 2023.
- [15] A. Amoozandeh Nobaveh, G. Radaelli, and J. L. Herder, "A Design Tool for Passive Wrist Support," in *Wearable Robotics: Challenges and Trends*, Cham, 2022, pp. 13-17: Springer International Publishing.
- [16] A. Seth, M. Dong, R. Matias, and S. Delp, "Muscle Contributions to Upper-Extremity Movement and Work From a Musculoskeletal Model of the Human Shoulder," (in English), Original Research vol. 13, 2019-November-05 2019.
- [17] T. Järvinen, M. Kääriäinen, M. Järvinen, and H. Kalimo, "Muscle strain injuries," *Current opinion in rheumatology*, vol. 12, pp. 155-61, 04/01 2000.
- [18] M. Moerman, "Lateral torsional buckling in translational and rotational compliant joints to obtain zero-stiffness behaviour," *Master thesis in TU Delft, under embargo*, 2023.

- [19] H. J. Hermens, B. Freriks, C. Disselhorst-Klug, and G. Rau, "Development of recommendations for SEMG sensors and sensor placement procedures," *Journal of Electromyography and Kinesiology*, Article vol. 10, no. 5, pp. 361-374, 2000.
- [20] M. B. I. Reaz, M. S. Hussain, and F. Mohd-Yasin, "Techniques of EMG signal analysis: Detection, processing, classification and applications," *Biological Procedures Online*, Article vol. 8, no. 1, pp. 11-35, 2006.

Appendix I. Implementation

1. Implementation of the design tool

1.1 Simulate the mechanical behavior of the exoskeleton

The distortion of the exoskeleton beam is caused by the displacement of its endpoints, which are the 2 interfaces between the exoskeleton and user in simplified assumption, moving from their resting locations to their new locations with arm movements. As the interfaces are assumed to connect rigidly with the user's upper arm and lower back, the path of them can be retrieved from the marker traces during arm elevation movement. In OpenSim model, the marker on humerus center is selected as the upper arm interface location. In the case study, the back interface is assumed to be still to simplify work, while a marker on lower back can also be selected to represent it for more realistic assumption.

5 “active” frames are selected from a full range arm elevation motion to represent arm elevated to different angles and the exoskeleton beam is deformed, and 1 “initial” frame is selected to represent the initial posture, where arm holds up vertically and the exoskeleton beam is not deformed. The location of the humerus center marker in these 6 frames can then be obtained. The difference between the marker position in 5 active frames and the initial frame tells the movement of the beam endpoint, the therefore the change in beam's boundary conditions. Beam deformation can be calculated after feeding this boundary condition to the FEA. The output includes the deformed beam shape and reaction force and moment on two endpoints of the beam, which acts on the user via interfaces.

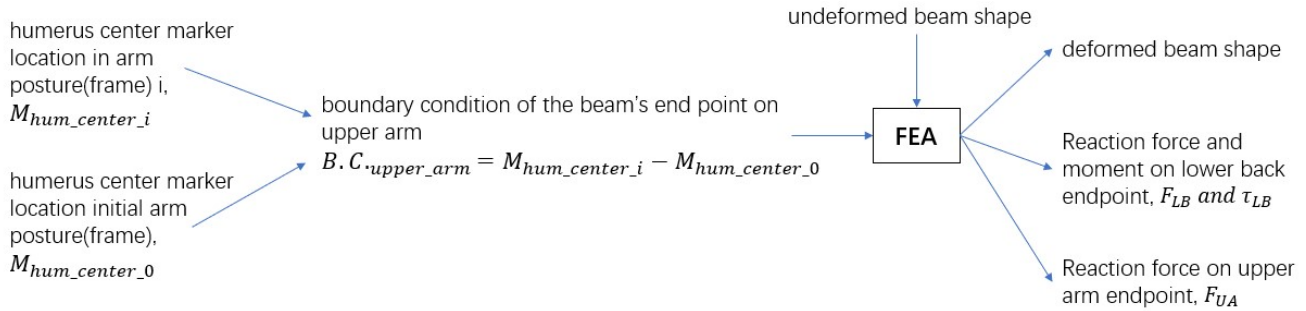


Figure D1. Calculate beam deformation with the FEA

1.2 Simulate the biomechanical effects of the exoskeleton

The external force exerted on humerus from the exoskeleton is fed into the RMR solver to calculate muscle activation and joint reaction force. The external force is always exerted on the humerus-center marker with its direction described in global frame. As described in method section, the effect of an external force is calculated by:

$$p_{biom} = w_1 \Delta muscle_activation^2 + w_2 \Delta joint_force^2 + w_3 \Delta muscle_peaks + w_4 \Delta muscle_compensation$$

$$\Delta muscle_activation = \sqrt{\sum_{i=1}^{33} x_i^2} / \sqrt{\sum_{i=1}^{33} x_{0i}^2}$$

$$\Delta joint_force = \frac{\|F_{GH_joint}\|}{\|F_{GH_joint0}\|} \text{ if } \|F_{GH_joint}\| > \|F_{GH_joint0}\|, \text{ else } 0$$

$$\Delta muscle_peak = \sum_{i=1}^{33} (x_i - 0.3) \cdot (x_i > 0.3)$$

$$\Delta muscle_compensation = \sum_{i=1}^{33} (x_i - x_{0i} - 0.2) \cdot (x_i > x_{0i} + 0.2)$$

1.3 Penalty on beam strain

Material strain can be computed with the vertices $p_{m,n}$ on the undeformed beam shape and the vertices $p'_{m,n}$ on deformed beam shape, in which $m = 1, 2, 3, \dots, N_{node} - 1, n = 1, 2, 3, 4$.

The beam element between beam node m and beam node $m+1$ is beam element e . The tensile strain on edge i of beam element e is

$$\varepsilon_i = \frac{\|(p'_{m+1,n} - p'_{m,n}) - (p_{m+1,n} - p_{m,n})\|}{\|p_{m+1,n} - p_{m,n}\|} \cdot 100$$

If the tensile strain on any of the 4 edges is larger than 1, the tensile strain in beam element e , $\varepsilon_e = (\varepsilon_1, \varepsilon_2, \varepsilon_3, \varepsilon_4)$, else $\varepsilon_e = 0$

Penalty on high strain $p_{strain} = w_{strain} \sum_{e=1}^{50} \varepsilon_e$

If least friction on upper-arm interface is preferred, $p_{friction} = w_{friction} \|F_{along_arm}\|$ can be added to the objective function, as friction mainly depends on the level of the along-arm part of the assistive force.

1.4 Selection of optimizer

Fmincon with interior point was initially selected to optimize the problem, following suggestions from previous works. Multistart was used to start the local optimization from different points, so that more parameter space can be covered. The optimization was finally completed with Genetic Algorithm for the convenience of using parallel computing. Population was 1000 as best solution usually converges while increasing population size from 1000.

2. Replacing the biomechanical simulation with a look-up table

As calling RMR solver takes relatively much longer time than computing beam deformation, involving it will significantly decrease optimization speed. It is also temporarily not compatible with the parallel computing platform. A solution for these is to create a look-up table with muscle activation and joint reaction force under different external forces and different arm postures. Visualizing this look-up table also shows how muscle activation varies with external loading and gives more insight in assistive device design.

External forces are reconstructed from global frame to an upper-arm frame (different than humerus frame in OpenSim). A force is decomposed to three parts: a force in alignment with the upper arm, defined by the line from humerus head center to elbow center, a force perpendicular to the upper arm and generating anti-gravity torque, and a force perpendicular to the upper arm and gravity direction (in horizontal abduction direction). This decomposition method expresses external forces in a more biomechanical manner and enables the observation to the effects of each force component.

Vector representing upper arm direction: $v_{arm} = \frac{x_{elbowcenter} - x_{humerushead}}{\|x_{elbowcenter} - x_{humerusheadcent}\|}$, $F_{aa} = F \cdot v_{arm}$

Vector representing the vertical direction: $v_{vert} = (0 \ 1 \ 0)$, $F_g = F \cdot v_{vert}$

Vector representing the horizontal abduction direction: $v_{lat} = v_{arm} \times v_{vert}$, $F_{lat} = F \cdot v_{lat}$

As the look-up table should not be unnecessarily large and the exoskeleton should neither generate excessively large force in any configuration, the look-up table is determined to span $[-28, 30] \times [0, 140] \times [-48, 30]$ (FaaxFagxFlat) with a resolution of 2N.

When the assistive force (Fx Fy Fz) from the beam is passed from FEM, it needs to be interpolated to get the corresponding muscle activation and joint reaction force.

The force is first reconstructed from (Fx Fy Fz) to (Fg Flat Faa), and interpolated from its 8 surrounding points in the look-up table:

$$\begin{aligned}
p_1 &= \left(\text{floor} \left(\frac{F_g}{2} \right) * 2, \quad \text{floor} \left(\frac{F_{lat}}{2} \right) * 2, \quad \text{floor} \left(\frac{F_{aa}}{2} \right) * 2 \right) \\
p_2 &= \left(\text{floor} \left(\frac{F_g}{2} \right) * 2, \quad \text{floor} \left(\frac{F_{lat}}{2} \right) * 2, \quad \text{ceil} \left(\frac{F_{aa}}{2} \right) * 2 \right) \\
p_3 &= \left(\text{floor} \left(\frac{F_g}{2} \right) * 2, \quad \text{ceil} \left(\frac{F_{lat}}{2} \right) * 2, \quad \text{floor} \left(\frac{F_{aa}}{2} \right) * 2 \right) \\
p_4 &= \left(\text{floor} \left(\frac{F_g}{2} \right) * 2, \quad \text{ceil} \left(\frac{F_{lat}}{2} \right) * 2, \quad \text{ceil} \left(\frac{F_{aa}}{2} \right) * 2 \right) \\
p_5 &= \left(\text{ceil} \left(\frac{F_g}{2} \right) * 2, \quad \text{floor} \left(\frac{F_{lat}}{2} \right) * 2, \quad \text{floor} \left(\frac{F_{aa}}{2} \right) * 2 \right) \\
p_6 &= \left(\text{ceil} \left(\frac{F_g}{2} \right) * 2, \quad \text{floor} \left(\frac{F_{lat}}{2} \right) * 2, \quad \text{ceil} \left(\frac{F_{aa}}{2} \right) * 2 \right) \\
p_7 &= \left(\text{ceil} \left(\frac{F_g}{2} \right) * 2, \quad \text{ceil} \left(\frac{F_{lat}}{2} \right) * 2, \quad \text{floor} \left(\frac{F_{aa}}{2} \right) * 2 \right) \\
p_8 &= \left(\text{ceil} \left(\frac{F_g}{2} \right) * 2, \quad \text{ceil} \left(\frac{F_{lat}}{2} \right) * 2, \quad \text{ceil} \left(\frac{F_{aa}}{2} \right) * 2 \right)
\end{aligned}$$

Muscle activation under this force is $\sum_{i=1}^8 \text{muscle}E(p_i)$, and joint reaction force is $\sum_{i=1}^8 \text{joint}F(p_i)$.

When the exoskeleton force is within this range, the biomechanical effect part in penalty is calculated in the way defined as section 1.2 with the interpolated muscle activation and joint reaction force. Otherwise, it is calculated by

$$\begin{aligned}
F'_g &= \{0, \quad \text{if } F_g < 0 \text{ } 140, \quad \text{if } F_g > 140 \text{ } F_g, \quad \text{if } 0 \leq F_g \leq 140 \\
F'_{lat} &= \{-48, \quad \text{if } F_{lat} < -48 \text{ } 30, \quad \text{if } F_{lat} > 30 \text{ } F_{lat}, \quad \text{if } -48 \leq F_{lat} \leq 30 \\
F'_{aa} &= \{-28, \quad \text{if } F_{aa} < -28 \text{ } 30, \quad \text{if } F_{aa} > 30 \text{ } F_{aa}, \quad \text{if } -28 \leq F_{aa} \leq 30
\end{aligned}$$

The muscle activation and joint reaction force under the new force $(F'_g, F'_{lat}, F'_{aa})$, with the interpolation method described in (.). In addition to the penalty to the biomechanical effects of this new force, the part of the original force exceeding the look-up table boundary is penalized by

$$\begin{aligned}
\text{penalty}_{excessive} &= w_1 F_{g-excessive} + w_2 F_{lat-excessiv} + w_3 F_{aa-excessive} \\
\text{in which } F_{g-excessive} &= \{F_g - 140, \text{if } F_g > 140 - F_g, \text{if } F_g < 0, \\
F_{lat-excessiv} &= \{F_{lat} - 30, \text{if } F_{lat} > 30 - 48 - F_{lat}, \text{if } F_{lat} < -48, \\
F_{aa-excessive} &= \{F_{aa} - 30, \text{if } F_{aa} > 30 - 28 - F_{aa}, \text{if } F_{aa} < -28
\end{aligned}$$

as excessively large external force is devastating to human body and should be avoided by imposing high penalty. Interference and material strain parts in penalty are calculated in the same way.

3. Simulated robustness test

Simulating the performance of the designed exoskeletons in perturbed movements first needs a motion file of perturbed arm elevation. The perturbation is added to the plane of elevation and the angle of arm elevation by -10deg to 10deg each with a resolution of 0.5deg. A new motion file with 41*41=1681 postures is generated, and it is used to repeat the process described in section 1.1 and 1.2. With the resultant muscle activation and joint reaction, maps depicting the biomechanical effects of the 2 designed exoskeletons under perturbation are obtained to reflect the robustness of the exoskeletons.

Appendix II. Dimension of exoskeleton beam designs

Table D1

Design	Control point location[x y z]	Cross section [H W]	Cross section orientation about guide curve[deg]	Clamp angle[deg]
1	-0.0240 0.0636 0	0.0224 0.0175	32.7191	-66.3736
	-0.0189 0.1669 0.0357	0.0109 0.0193	11.3589	38.7643
	-0.0255 0.2031 -0.0110	0.0040 0.0011	160.8151	
	-0.0148 0.2500 0.0460	0.0028 0.0067	80.5621	
	0.0087 0.2618 0.0963	0.0056 0.0063	167.1438	
	0.0232 0.3495 0.1149	0.0044 0.0012	134.5713	
	0.0790 0.4114 0.0574	0.0102 0.0014	112.4584	
2	-0.0249 0.0619 0	0.0173 0.0129	137.4861	49.7102
	-0.0498 0.1770 -0.0254	0.0025 0.0089	115.3298	48.6758
	-0.0251 0.1913 0.0526	0.0059 0.0085	164.6841	
	0.0020 0.2109 0.0987	0.0030 0.0087	138.6683	
	0.0075 0.3143 0.0939	0.0032 0.0073	161.7857	
	0.0269 0.3156 0.1268	0.0032 0.0047	153.8955	
	0.0790 0.4114 0.0574	0.0049 0.0020	160.0673	
3	-0.0174 0.0725 0	0.0157 0.0048	120.2656	27.0419
	-0.0029 0.1669 -0.0077	0.0116 0.0047	149.7921	32.0922
	-0.0297 0.2313 0.0732	0.0077 0.0026	159.0781	
	-0.0245 0.3134 0.0873	0.0083 0.0028	166.1907	
	0.0012 0.2964 0.0931	0.0078 0.0009	159.2101	
	0.0439 0.4261 0.1288	0.0064 0.0047	94.2608	
	0.0790 0.4114 0.0574	0.0079 0.0013	92.8853	
4	-0.0220 0.0239 0	0.0076 0.0230	72.8704	22.0147
	-0.0201 0.1646 0.0078	0.0100 0.0060	58.7007	39.7903
	-0.0187 0.1855 0.0158	0.0030 0.0078	100.9693	
	-0.0237 0.2119 0.0997	0.0041 0.0094	107.2957	
	0.0116 0.2648 0.1291	0.0013 0.0077	169.1792	
	0.0222 0.3218 0.1317	0.0030 0.0037	151.1845	
	0.0790 0.4114 0.0574	0.0046 0.0028	159.7302	
5	-0.0293 0.0774 0	0.0245 0.0063	83.9972	78.1256
	-0.0204 0.1897 -0.0021	0.0020 0.0122	77.8005	42.5313
	-0.0250 0.2432 0.0118	0.0042 0.0038	132.7118	
	-0.0179 0.2204 0.1150	0.0030 0.0106	150.8501	
	0.0014 0.2686 0.1347	0.0020 0.0047	114.7828	
	0.0656 0.3133 0.1227	0.0040 0.0033	169.9906	
	0.0790 0.4114 0.0574	0.0029 0.0043	169.9705	
6	-0.0255 0.0937 0	0.0052 0.0167	97.5060	-29.0117
	0.0118 0.1566 0.0466	0.0042 0.0172	119.5781	58.9201
	-0.0277 0.1898 0.0509	0.0066 0.0068	143.1816	
	-0.0168 0.2465 0.0646	0.0019 0.0109	137.5386	
	0.0013 0.2933 0.0949	0.0023 0.0030	151.6221	
	0.0051 0.3941 0.0673	0.0028 0.0026	144.3868	
	0.0790 0.4114 0.0574	0.0079 0.0039	133.9357	

Table D2. In design 3 and design 6, dislocation of lower back interface by servomotor per arm posture

Design	Posture 1[Δy Δz]	Posture 2[Δy Δz]	Posture 3[Δy Δz]	Posture 4[Δy Δz]	Posture 5[Δy Δz]
3	-0.0036 0.0187	-0.0326 0.0108	-0.0682 0.0162	NA	NA
6	-0.0039 0.0859	0.0578 -0.0184	0.0534 0.0202	-0.0183 0.0990	-0.0642 0.0283

Appendix III. Modeling the exoskeleton assisted task on a male model

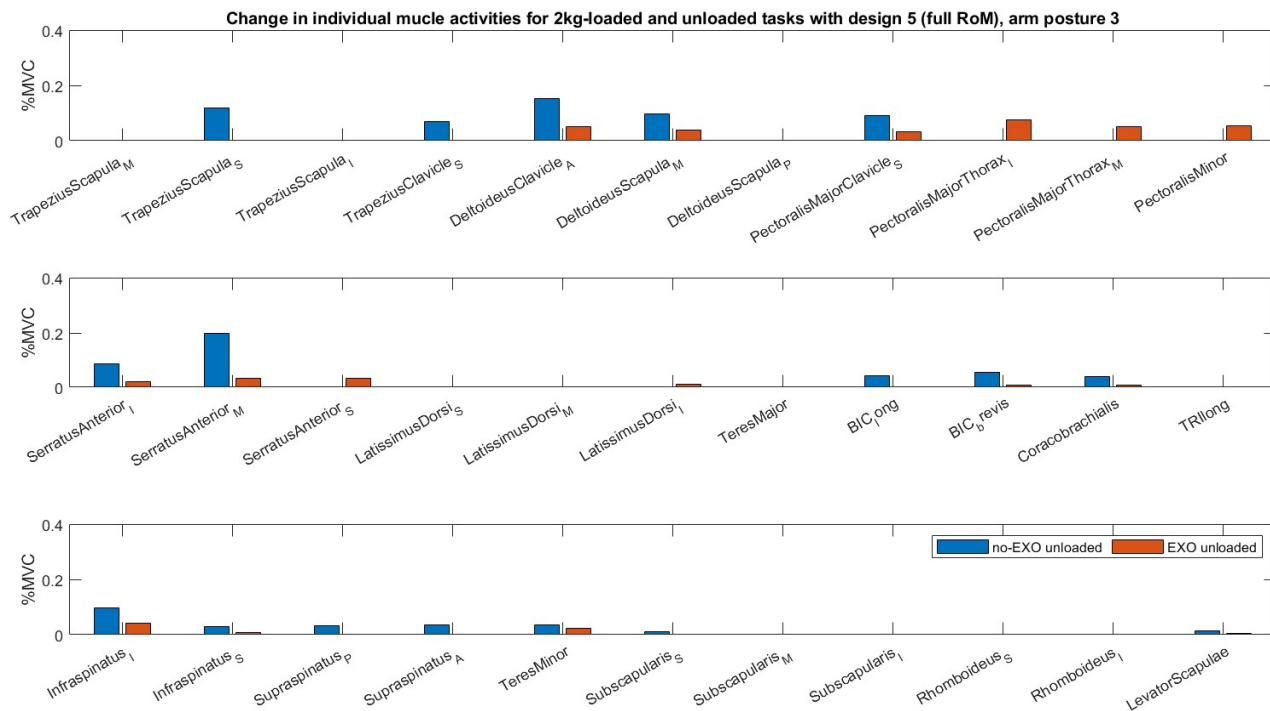


Figure D2. Effects of exoskeleton-equivalent forces from design 2 on a male shoulder model

The male model was scaled up in bone lengths and the mass from the smaller model used in the design procedure. Bone lengths were scaled up to the height of average adult male with reference to the length of the sternum. The mass was scaled up in a way that the body mass index($mass/(height^2)$) of the model was unchanged. The muscle activities computed by the RMR solver show that the exoskeleton-equivalent force of design 2 in arm posture 3 induces muscle compensation in pectoralis major thorax, which is not coherent to the experiment result.